FABRICATION OF ZINC OXIDE/GRAPHENE OXIDE POLYSULFONE MIXED MATRIX MEMBRANES FOR CADMIUM IONS ADSORPTION

CHOO YUNG LIM

A project report submitted in partial fulfilment of the requirements for the award of Bachelor of Engineering (Hons.) Chemical Engineering

Lee Kong Chian Faculty of Engineering and Science
Universiti Tunku Abdul Rahman

August 2018

DECLARATION

I hereby declare that this project report is based on my original work except for citations and quotations which have been duly acknowledged. I also declare that it has not been previously and concurrently submitted for any other degree or award at UTAR or other institutions.

Signature : _____

Name : Choo Yung Lim

ID No. : 1406574

Date : _____

APPROVAL FOR SUBMISSION

I certify that this project report entitled **"FABRICATION OF ZINC OXIDE/GRAPHENE OXIDE POLYSULFONE MIXED MATRIX MEMBRANES FOR CADMIUM IONS ADSORPTION"** was prepared by **CHOO YUNG LIM** has met the required standard for submission in partial fulfilment of the requirements for the award of Bachelor of Engineering (Hons.) Chemical Engineering at Universiti Tunku Abdul Rahman.

Approved by,

Signature : _____

Supervisor : Ms. Chong Woon Chan

Date : _____

Signature : _____

Co-Supervisor : Dr. Pang Yean Ling

Date : _____

ACKNOWLEDGEMENTS

I would like to thank everyone who had contributed to the successful completion of this project especially, Dr. Lee Khia Min's master student Mr. Ong Ching Yeh and Dr. Mah Shee Keat's master student Mr. Lim Su Wei for providing more than enough assistance in carrying out this research. Without their guidance and knowledge, this research would have not come to a completion.

Moreover, I would like to express my gratitude to my research supervisor, Ms. Chong Woon Chan for her invaluable advice, guidance and her enormous patience throughout the development of the research. She had pin pointed my mistakes which led to me to further improve my thesis quality.

In addition, I would also like to express my gratitude to my loving parents and friends who had helped and given me encouragement throughout this period.

ABSTRACT

Excessive heavy metal ions in wastewater should be removed to ensure the reuse of effluent from the treated wastewater by industries in order for them to maintain their daily production processes. In this study, the potential of employing zinc oxide/graphene oxide polysulfone mixed matrix membranes (ZnO/GO PSF MMMs) to remove cadmium ions was studied. Neat PSF membranes and 1 wt% ZnO/GO PSF MMMs were fabricated by using the phase inversion method in this research. Scanning electron microscopy (SEM) with an energy dispersive X-ray spectroscopy (EDX), Fourier-tansform Infrared spectroscopy (FTIR) and inductively coupled plasma optical emission spectroscopy (ICP-OES) were applied in this research for studying the characterization and composition of the membranes. Parameters such as pH, contact time, initial feed concentration, the presence of humic acid and the number of membranes had been studied. From the results, the optimum pH value for the Cd^{2+} adsorption is pH 5.5 and the optimum contact time was 3 hours. In addition, the optimum initial concentration of Cd^{2+} was 25 ppm and the increasing number of membranes will lead to higher adsorption capacity. Besides that, the amount of adsorbed Cd^{2+} on the membranes was greatly reduced when humic acid existed in the heavy metal solution. The adsorption data satisfactorily fitted to Langmuir and pseudo-second order models. According to Langmuir adsorption isotherm, the q_{max} obtained was 0.000698 mg/cm^2 and the Langmuir constant of adsorption was 0.2227 L/mg. According to pseudo-second order kinetic model, the q_{eq} obtained was 0.00073 mg/cm^2 and the rate constant for pseudo-second order was 964.3 cm^2/mg.h at 25 ppm of Cd^{2+} solution. The result from the three cycles of desorption and regeneration had proven that ZnO/GO PSF MMM showed good desorption performance. The bulk analysis showed that the adsorbed Cd^{2+} in membrane per weight of ZnO/GO is higher than the adsorbed Cd^{2+} in bulk per weight of ZnO/GO because nano-adsorbents in the suspension will cause the agglomeration in aqueous solution during the adsorption process.

TABLE OF CONTENTS

LIST OF TABLES

LIST OF FIGURES

LIST OF SYMBOLS / ABBREVIATIONS

b	Langmuir constants of adsorption
C_1	concentration of Cd^{2+} stock solution, ppm
C_2	desired concentration of Cd^{2+} stock solution, ppm
Ce	equilibrium concentration of metal ions in solution, mg/L
C_o	initial concentration of metal ions in solution, mg/L
k_1	rate constant for pseudo first order, 1/min
k_2	rate constant for pseudo seconds order, g/mg.min
m	weight of adsorbent, g
q_e	adsorption capacity, mg/g
q_{eq}	equilibrium adsorption capacity, mg/g
q_{max}	maximum adsorption capacity, mg/g
q_t	adsorption capacity at time t, mg/g
t	time, min
V	volume of the solution, L
V_1	volume of Cd^{2+} stock solution required for dilution, mL
V_2	desired volume of Cd^{2+} stock solution, mL
CNT	Carbon Nanotube
FTIR	Fourier-Transform Infrared Spectroscopy
ICP-OES	Inductively Coupled Plasma Optical Emission Spectroscopy
IPDI	Isophorone Diisocyanate
MMM	Mixed Matrix Membrane
NMP	N-Methyl-2-pyrrolidone
PSF	Polysulfone
PES	Polyethersulfone
ppm	parts per million
PVDF	Polyvinylidene fluoride
SEM	Scanning Electron Microscope
TMP	Trans membrane pressure

LIST OF APPENDICES

CHAPTER 1

INTRODUCTION

1.1 Background

The request for new water resources has getting desperate worldwide due to the rapid growth of world population and increment of water demand. Reuse of effluent from the treated wastewater is essential for many industries in order for them to maintain their daily production processes (Richards et al., 2012).

A large quantity of heavy metals is discharged into water bodies such as lakes and rivers on daily basis from large industrial activities, for example, mining, car manufacturing and electroplating. Heavy metals are not just toxic, they are also non-biodegradable. They will gather inside our bodies and food chain and lead to significant health and environmental problems (Al-Malack and Basaleh, 2016). There are a lot of negative effects of heavy metals, for instance, emphysema, renal damage, hypertension and skeletal malformation in foetuses (Pourbeyram, 2016). For example, cadmium ions, Cd^{2+} are highly toxic to humans and they are the sixth most poisonous substance that affect human health. Cd^{2+} can be introduced into bodies of water such as rivers and lakes from various sources, for instance, smelting, metal plating, phosphate fertilizers, pigments, alloy industries, mining, stabilizers, and sewage sludge. The negative effects of an excess of Cd^{2+} ions involve several acute and chronic disorders, for example, vomiting, diarrhoea, abdominal pain, and testicular atrophy (Khan et al., 2013).

There are plenty of processes for the application of heavy metal removals such as ion exchange, irradiation, oxidation, photochemical, electrochemical treatment, membrane, adsorption and the others as shown in Table 1.1 (Fu and Wang, 2011). Among them, adsorption is recognized as an economic and effective way for the application of heavy metal removal. Adsorption is a mass transfer process and substances bounded by chemical and physical interactions to the solid surface (Gunatilake, 2015). Adsorption is commonly used because it is easy to perform, flexible in design and operation, insensitive to toxic substances, reversible and the adsorbents could be regenerated by appropriate desorption process (Pourbeyram, 2016).

Table 1.1: The Advantages and Disadvantages of Different Treatment Technologies for Removal of Heavy Metal (Ariffin et al., 2017)

Treatment Technologies	Advantages	Disadvantages
Oxidation	Fast process	Formation of by-products and high energy costs
Adsorption	Simplicity and flexibility of design, insensitivity to toxic pollutants and ease of operation	Adsorbents need regeneration
Ion exchange	Wide range of heavy metals can be removed	Adsorbents need regeneration
Membrane filtration	A variety of heavy metals can be removed	Expensive and produce of concentrated sludge
Ozonation	Can be applied in gaseous state	Half life is short
Coagulation/flocculation	Cost effective	Production of sludge is high and big size particles will be formed
Electrochemical treatment	Process is rapid and good for the removal of particular metal ions.	Cost ineffective and big size particles will be formed

Biological treatment	Effective for the removal of some metals	Technology is not yet to be commercialized and established
Fentons reagent	Energy input is not necessary for the activation of the hydrogen peroxide and capable of treating a variety of wastes	Sludge is generated
Electrokinetic coagulation	Economically feasible	High production of sludge
Irradiation	Good at lab scale	A lot of dissolved oxygen are required
Photochemical	No production of sludge	By-product is formed

The processes of membrane separation have been used intensively in wastewater treatment. Polysulfone (PSF) membrane is one of the most general membranes that has been used in ultrafiltration of wastewater because of its high thermal resistance, mechanical stability and excellent film-forming properties (Richards et al., 2012). The disadvantage of this membrane is that its hydrophobicity will cause membrane fouling. The membrane fouling is caused by deposition of organic pollutants in water onto membrane surface. These pollutants are mainly hydrophobic in nature. A lot of researches have been conducted to improve the hydrophilicity of the PSF membranes. Therefore, metal oxide nanoparticles are introduced recently to the polymer matrix to reduce membrane fouling problem by increasing its hydrophilicity (Phelane, 2013).

Recently, nano-adsorbents as an effective adsorbent has become a research hotspot due to its large surface area-to-volume ratio and high interfacial activity. Nano zinc oxide (ZnO) is an important inorganic functional material in which it shows high adsorption capacity for H_2, CO and CO_2. Nano ZnO is more cost effective than the other commonly used nano-adsorbents, for instance, Al_2O_3 and TiO_2 nanoparticles

(Zhang et al., 2014). Besides that, graphene oxide (GO) has been widely used in many fields, such as medicine, electrode modification and environmental application due to its special properties and structure (Zhang et al(a)., 2017). Graphene oxide (GO) is an oxidized graphene with different oxygenated functionalities, for example, carbonyl and carboxylic acid at the edges, and hydroxyl and epoxy on the basal plane. The metal ions can bind efficiently on the surface of GO through the sharing of the lone pair of electron on the oxygen, therefore causing it an adsorbent that can remove heavy metal ions efficiently (Mukherjee et al., 2016).

In this research, the effect of ZnO/GO incorporated into the PSF membranes to form zinc oxide/graphene oxide mixed matrix membranes, ZnO/GO PSF MMMs for cadmium ions, Cd(II) adsorption was first investigated. Mixed matrix membrane is classified as a composite membrane where one or more inorganic additives are distributed in the polymeric matrix. The introduction of inorganic additives provides a few benefits such as higher surface charge and adsorption capacity resulting in enhanced rejection of heavy metal ions while maintaining high permeate flux (Mukherjee et al., 2016). The functionalization of GO onto ZnO was to show a better distribution of nano-adsorbents and prevent the agglomeration of ZnO due to high negatively charged GO sheets that lead to strong repulsive effects (Peng et al., 2017).

1.2 Problem Statement

According to Kolbasov et al. (2017), over four billion people in the world will live without a sufficient source of clean water by the year 2025. One of the reasons of water shortage is due to continuous pollution of water sources such as lakes and rivers with heavy metals by industrial activities such as mining, alloys and steel manufacturing, metallurgical, electroplating, electronics, etc. (Kolbasov et al., 2017). As the heavy metals are non-degradable, they will remain in the environment for an extremely long time. Hence, remediation steps must be carried out to rectify this problem.

Various wastewater treatment techniques have been proposed and used in the past, for example, biological treatment, adsorption, ion exchange, ozonation, chemical reduction/oxidation, electrodialysis and others (Kolbasov et al., 2017). Recently, the adsorption method by using nano-adsorbents has been focused because it is cheaper and efficient for the application of heavy metal removal. Nano-adsorbents in the suspension will cause the agglomeration in aqueous solution during the adsorption process in spite of the fact that they are cost effective and these nano-adsorbents are

hard to be regenerated from the water. Therefore, it has been proposed that the combination of membrane separation process and adsorption can overcome the problems of difficult regeneration and agglomeration of nano-adsorbents (Koushkbaghi et al., 2017)

This study represents the overview of adsorption of cadmium ions, Cd^{2+} by using ZnO/GO PSF MMMs under various different conditions. The main reason for adding ZnO to GO was targeted for better dispersion of ZnO in the polymer matrix.

1.3 Aims and Objectives

This study is to fabricate zinc oxide/graphene oxide polysulfone mixed matrix membranes (ZnO/GO PSF MMMs) and study its adsorption behaviour. The main objectives of this study include:

(i) To fabricate and characterize the neat PSF membranes and ZnO/GO PSF MMMs.

(ii) To study the adsorption performance of cadmium ions, Cd^{2+} by ZnO/GO PSF MMMs under different pH conditions, contact time, number of membranes and initial concentration of Cd^{2+}.

(iii) To study the adsorption performance of Cd^{2+} by ZnO/GO PSF MMMs with the addition of an organic matter, humic acid under the optimum condition.

(iv) To determine the adsorption model for Cd^{2+} adsorption using ZnO/GO PSF MMMs.

(v) To study the desorption and regeneration of the ZnO/GO PSF MMM under the optimum condition.

(vi) To study the adsorption performance of the ZnO/GO in both MMMs and bulk.

1.4 Scopes

The conduction of this study is to fabricate ZnO/GO PSF MMMs and study its adsorption performance under different operating conditions such as pH, contact time, number of membranes and initial concentration of cadmium ions, Cd^{2+}. ZnO/GO PSF MMMs were prepared by dispersing the ZnO/GO composite in PSF casting solutions (N-methyl-2-pyrrolidone (NMP) as solvent). Then, morphologies and composition of ZnO/GO PSF MMMs were characterized by SEM-EDX.

The ZnO/GO PSF MMMs were placed in the solutions containing Cd^{2+} ions for a certain period of time. The initial and final concentration of Cd^{2+} ions in the solution were then identified using Inductively Coupled Plasma Optical Emission Spectroscopy (ICP-OES). Different initial concentrations of Cd^{2+} were used to study the adsorption performance by the ZnO/GO PSF MMMs. By adjusting the pH values of Cd^{2+} solutions, the adsorption ability of ZnO/GO PSF MMMs at different pH conditions were evaluated. The adsorption ability of ZnO/GO PSF MMMs can also be identified at different contact time. Moreover, the adsorption performance was identified by using different number of membranes. With the addition of an organic matter, humic acid under optimum condition, the adsorption performance by ZnO/GO PSF MMMs were studied. The data and results obtained from the experiment were interpreted to determine the suitability of adsorption model for Cd^{2+} adsorption using ZnO/GO PSF MMMs. The performance of desorption and regeneration of the membrane under the optimum condition was also evaluated. In addition, the adsorption performance of the ZnO/GO in both MMMs and bulk was also studied. All the information and details are reported in Chapter 4 (Results and Discussion).

CHAPTER 2

LITERATURE REVIEW

2.1 Heavy Metal

Heavy metals are metals or materials which density exceeds 5 g per cubic centimetre. Heavy metals will lead to negative health effects such as reduced growth, cancer, nervous system damage and even death (Barakat, 2011). Besides that, exposure to certain heavy metals, for example, mercury and lead might cause the development of autoimmunity, in which a person's own cells attacked by its own immune system. This can cause joint diseases such as rheumatoid arthritis, diseases of the kidneys, nervous system, circulatory system and damage to the fetal brain. Besides that, heavy metals can cause irreversible damage to the brain at higher doses. For example, as children consume more food for their body weight than the adults, they might receive higher doses of metals from food than the adults (Barakat, 2011). Table 2.1 shows some of the heavy metals that are currently in the environment, their sources and also their effects on human beings.

Table 2.1: Sources and Effects of Heavy Metals (Ariffin et al., 2017)

Heavy Metal	Sources	Effects
Copper	Water heaters, fungicides, hormone pills, pesticides, beverages from copper brewery equipment, water pipes and instant gas hot water heaters.	Nausea/vomiting, autism, stuttering, arthritis, hypertension, mental disorder, anaemia, hyperactivity, enlargement and inflammation of liver, cystic fibrosis and heart problem

Nickel	Effluents of zinc base casting, storage battery industries, silver refineries and electroplating	Cancer of nose, lungs and bone, headache, dermatis, myocarditis, pulmonary fibrosis, dizziness and nausea
Chromium	Textile and steel industry	Respiratory problems, skin rashes, haemolysis, liver damage and lung cancer
Lead	Steel, mining, batteries, automobile and paints industries	Headache and vomiting, nausea, hyperactivity, mental retardation, thyroid dysfunction, fatigue and anorexia
Mercury	Industries such as oil refining, rubber processing and fertilizer, paints, batteries, fabric softeners, cosmetic and pharmaceuticals	Birth defects, tremors, gingivitis, chromosome damage, mental retardation, nausea, seizures, tooth loss and loss of hearing of vision
Cadmium	Cadmium-nickel batteries, metal plating, mining, pigments, stabilizers, phosphate fertilizers and alloys	Hypertension, testicular atrophy, emphysema, renal damage and itai-itai disease

2.2 Adsorption Mechanism

Ion exchange, electrostatic attraction and surface complexation were found to be the adsorption mechanisms of heavy metal ions on the surface of GO (Peng et al., 2017). The molecular structure of GO is presented in Figure 2.1. GO contains functional groups such as OH, -COOH, -O- and C=O, giving more reaction possibilities (Yakout et al., 2017). The adsorption mechanism of heavy metal ions for ZnO nanoparticles might mainly due to both electrostatic attraction and ion exchange (Zito Ray and J. Shipley, 2015).

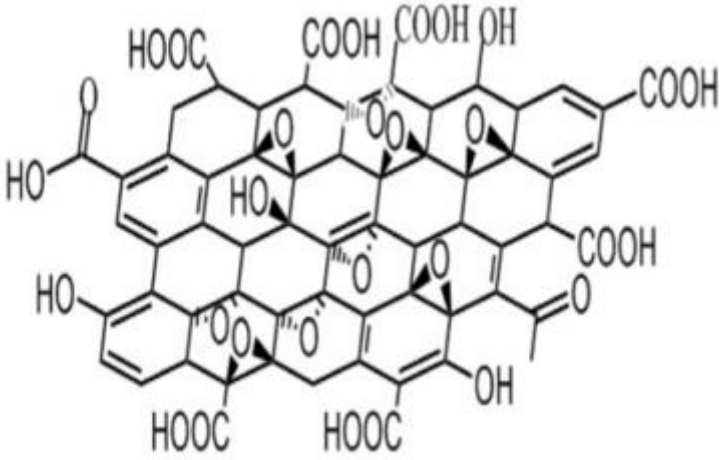

Figure 2.1: Structure of GO (Peng et al., 2017).

2.2.1 Ion Exchange

The reaction between heavy metal ions and the proton on the oxygenous groups for both the GO and ZnO such as -COOH or -OH is called ion exchange. It is one of the main adsorption mechanism and it is a reversible and fast process. The exchange of heavy metal cations and H^+ on the oxygenous groups were responsible for the adsorption process (Peng et al., 2017). Figure 2.2 shows the ion exchange reaction between Pb(II) and the proton on -COOH or –OH oxygenous function groups in GO.

$$-COOH + Pb^{2+} \longrightarrow -COOPb^{+} + H^{+}$$

$$-OH + Pb^{2+} \longrightarrow -O\,Pb^{2+} + H^{+}$$

Figure 2.2: Ion Exchange Reaction between Proton and Pb(II) on –OH or –COOH Oxygenous Function Groups in GO (Peng et al., 2017).

2.2.2 Electrostatic Attraction

The electrostatic attraction between the negatively charged ZnO/GO sheets and positively charged heavy metal ions produces a driving force for adsorption. The electrostatic interaction played a part in the adsorption process (Peng et al., 2017). Figure 2.3 shows the electrostatic attraction and ion exchange with heavy metal cations for GO.

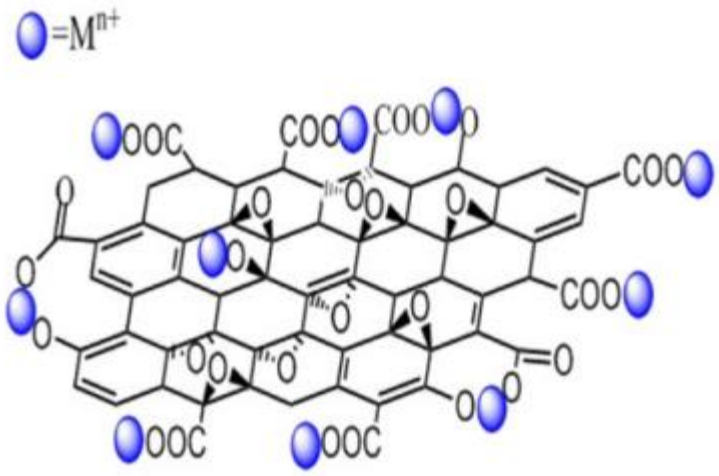

Figure 2.3: Electrostatic Attraction and Ion Exchange with Heavy Metal Cations for GO (Peng et al., 2017).

2.2.3 Surface Complexation

It was confirmed that the surface complexation between heavy metal ions and surface oxygenous functional groups had taken part in the adsorption of heavy metals on the surface of GO. For example, the oxygenous functional groups that have been located at the edges of GO sheets mainly participated in the complexation of Pb(II) and the Pb(II) bridged different GO sheets through simultaneously bonding the carboxyl groups or hydroxyl at the edges (Peng et al., 2017). Figure 2.4 shows the adsorption of heavy metal ions on GO through surface complexation.

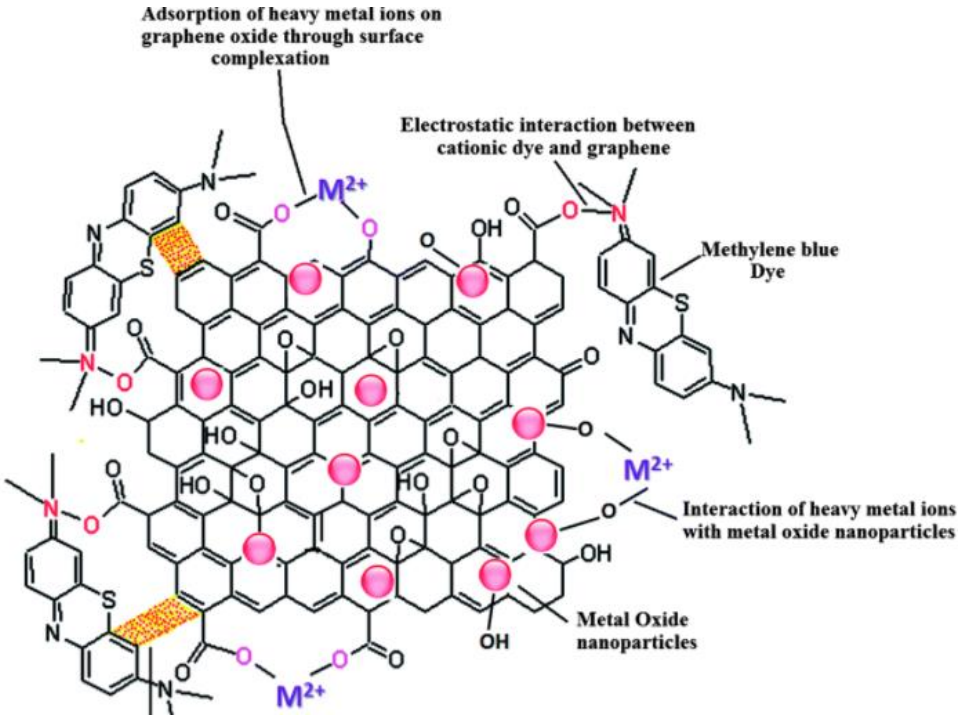

Figure 2.4: The Adsorption of Heavy Metal Ions on GO through Surface Complexation. (Upadhyay et al., 2014)

The surface complexation models are chemical models that give a molecular description of adsorption phenomena using an equilibrium approach. The consideration of the charges on both the adsorbing ion and solid adsorbent surfaces makes surface complexation models become one of the major advancements (Goldberg, 2013). Surface complexation models describe sorption depend on surface reaction equilibrium and there are basically three common surface complexation models such as the constant capacitance model (CCM), the diffuse layer model (DLM), and the triple layer model (TLM) (Li Li, 2018).

2.3 PSF Membrane

Polysulfone, PSF is an organic polymer that has been widely used due to its good chemical and thermal stability, excellent oxidative resistance and mechanical strength (Tiron et al., 2017). The chemical structure of PSF is shown in Figure 2.5. Polysulfone (PSF) membrane is a rigid, tough, transparent and high-strength thermoplastic that remains its characteristics over a wide range of temperatures (from −100 °C to over 160 °C) (Huang and Yang, 2006). They are resistant to chlorine oxidation, hence replacing cellulose acetate membrane which was once widely used for membrane fabrication (Majewska-Nowak, 1989).

PSF has been used as ion exchange membranes in electro-membrane processes such as polymer electrolyte membrane electrolysis and electrodialysis (Huang and Yang, 2006). Besides that, PSF is being used as a thermoplastic material in fabricating membranes for ultrafiltration systems (Huang and Yang, 2006).

A lot of studies have been carried out to enhance the hydrophilic properties of the PSF membrane surface. The process of blending with nanoparticles has become popular in the past decade because of their convenient operation and mild operating conditions. The process of blending can produce artificial membranes that have good separation performance, good chemical and thermal resistance. In addition, it also shows better adaptability to the conditions in harsh wastewater environments (Richards et al., 2012).

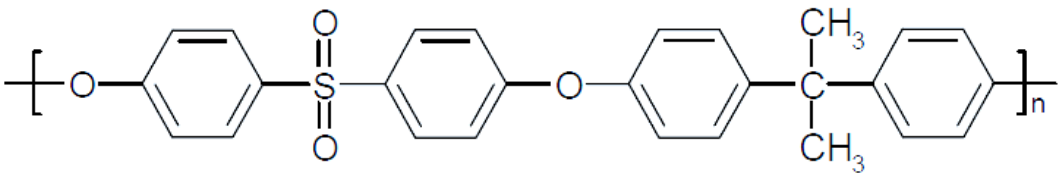

Figure 2.5: Chemical Structure of PSF (Polymerdatabase.com, 2018)

2.4 Adsorbents for Heavy Metal Ions Removal

2.4.1 Metal and Metal Oxides

Recently, metal and metal oxides such as zirconium (Zr), zinc oxide (ZnO), graphene oxide (GO), iron oxide (Fe_2O_3) and aluminium oxide (Al_2O_3) have been used as absorbents in the removal of heavy metal ions in the water and wastewater treatment. These materials showed good hydrophilicity, high flux recovery ratio, high adsorption capacity of heavy metal ions because of their high surface area-to-volume ratio as discussed in Section 1.1 (Mukherjee et al., 2016; Zhang et al(a)., 2017; Zhang et al., 2014; Yakout et al., 2017; Mondal et al., 2017). The modification and adsorption performance of various adsorbents such as metal and metal oxides, carbon source and natural source are summarized and presented in Table 2.2.

2.4.1.1 Zirconium

Zirconium is a metal cation that has high thermal stability and low toxicity. It's strong ionic and coordinative affinity towards the groups containing oxygen render it to be under study widely in the application of heavy metal ions removal in these recent years (Pourbeyram, 2016). According to the findings of Maximous et al. (2010), zirconium oxide/polyethersulfone (ZrO_2/PES) membrane and aluminium oxide/ polyethersulfone (Al_2O_3/PES) membrane showed high removal efficiencies for Pb(II), Cr(III) and Cd(II) under the operating conditions of pH 7 and low TMP of 0.69 bar. With the dosage of 5 % w/w metal oxides, the removal efficiency of Al_2O_3 for Pb(II) was almost similar to ZrO_2. For the removal of Cr (III), ZrO_2 had shown better removal efficiency which is 5.2 % more than Al_2O_3. For the removal of Cd(II), Al_2O_3 had shown better removal efficiency which is 2.2 % more than ZrO_2. As it can be seen, the removal efficiency of Al_2O_3 and ZrO_2 are quite similar and both of them are appropriate to be used for the application in the removal of Pb(II), Cr(III) and Cd(II) ions. The authors also mentioned that a smaller space requirement can be obtained by using the Al_2O_3/PES and ZrO_2/PES membrane comparing to the adsorption technique (using activated carbon, rice husk and maize leaves). Besides that, they have a lower maintenance cost and better control of membrane fouling (Maximous et al., 2010).

Table 2.2: Modification and Adsorption Performance of Various Adsorbents in MMMs or bulk

	Materials	Dosage	Main Findings Performance	Operational Parameters	Reference
			Metal and Metal Oxides		
1	Aluminium oxide/ polyethersulfone membrane, Al_2O_3/PES (MMM)	- 5 % w/w Al_2O_3 & 18 wt% PES polymer	- Removal efficiency: Pb(II): 99.3% Cr(III): 83.4% Cd(II): 13.2%	- pH: 7 - TMP : 0.69 bar	Maximous et al.,2010
2	Zirconium oxide/polyethersulfone membrane, ZrO_2/PES (MMM)	- 5% w/w ZrO & 18 wt% PES polymer	- Removal efficiencies: Pb(II): 99.5% Cr(III): 88.6% Cd(II): 11%	- pH: 7 - TMP : 0.69 bar	Maximous et al.,2010
3	Nickel iron oxide nanoparticle incorporated hollow fiber mixed matrix membrane (MMM)	- 3 wt% nanoparticle	- Maximum adsorption capacity: Lead: 52 mg/g Copper: 42 mg/g Zinc: 35 mg/g Cadmium: 24 mg/g Nickel: 17.5 mg/g	- pH: 7 - Initial heavy metal concentration: 50 mg/L - Cross flow rate: 20L/h. - TMP: 69 kPa	Mondal et al., 2017

			Chromium: 18 mg/g - More than 95% rejection for all heavy metal. - Regeneration: 0.1 N HCl solution for 10 h. - Contact angle: Dropped from 77° to 64°		
4	Zirconium-chitosan/graphene oxide membrane (MMM)	- 0.5 g Zr-CTS/GO	- Removal efficiency: Fluoride: (from 9.54 to 1.10 mg/L) HCO_3- : 153.75 to 29.09 mg/L SO_4^{2-} : 99.70 to 2.74 mg/L.	- pH: 7.39 - 50 mL of ground water sample - time: 60 min	Zhang et al(a)., 2017
5	Aminated-Fe_3O_4 nanoparticles filled chitosan/PVA/PES dual layers nanofibrous membrane (MMM)	- Aminated Fe_3-O_4 concentration (0-4 wt%)	- Maximum adsorption capacities: Cr(VI): 509.7 mg/g Pb(II) ions: 525.8 mg/g	- pH: 2-7 - Contact time: 0-60 min in batch - Initial concentration: 20-1000 mg/L in batch - Temperature: 30-50 °C in batch	Koushkbaghi et al., 2017

6	PVDF/ZnO hybrid membranes (MMM)	- 14 wt% PVDF - 2 wt% PVP - 3% ZnO	- Maximum adsorption capacity for Cu^{2+}: 87.4 ug/cm^2	- pH: 6 - Optimum equilibration time: 120 min - Initial concentration : 20 mg/L of Cu^{2+}	Zhang et al., 2014
7	Mixed metal oxide coated polymer beads composed of Fe-Ti bimetal oxides on a sulfonated polymer (B)	- 4-6 wt% of metal content - Fe content: 0.917 – 1.05 mmol/g bead. - Ti content: 0 to 66 μ mol/g bead.	- Selectivity factor>25 against background ions (e.g., CI-, NO3-, and SO_4^{2-}). - Maximum adsorption capacity: 7.14 to 59.0 mg-P/g metal with molar fraction of Ti to the total molar concentration of the two metals. (i.e., Fe and Ti) varied from 0 to 6%. - Regeneration: 97% phosphorus was recovered with 1.2 eq NaOH per L.	- Time: 48 h - Initial concentration: 5mg/L of P - Temperature: 25°C	Park et al., 2017

8	Zirconium metal-organic frameworks membrane (MMM)	- Maximum adsorption capacity: fluoride: 102.4 mg/g - Regeneration: 3 wt% sodium hydroxide solution - The fluoride removal abilities: 5510, 5173, and 4664 L/m^2 when fluoride concentrations were 5, 8 and 10 mg/L, respectively.	- pH: 7 - initial fluoride concentration: 200 mg/L	He et al., 2016

	Carbon Source				
9	Ceramic membrane and carbon nanotube (MMM)	- 0.2 µm of membrane	- Average adsorption capacities: Cadmium: 99.39% Mercury: 99.61% Nickel: 99.70% Cobalt: 99.72% Lead: 99.97% - Regeneration: A 2 wt% sodium hydroxide wash at 50 °C for 1 h, followed by a 1 % citric acid. 12% membrane flux recovery achieved.		Ainscough et al., 2017
10	Activated Carbon (B)		Removal Efficiency: - Pb (II): 98% - Cr(III): 95% - Cd(II): 83%	- pH 5 - Agitation	Maximous et al.,2010
11	Activated carbon produced from municipal organic solid waste (B)	- Surface area of 790 m^2/g - (25–300) mg per 50 mL of	- Removal efficiencies: Cd^{2+}: 78% Pb^{2+}: 94% - Maximum adsorption capacity:	- Temperature: 700˚C - Time: 2 h - pH: 3-7	Al-Malack and Basaleh, 2016

			metal solution	Cd^{2+}: 61 mg/g Pb^{2+}: 90 mg/g	- Contact time (0–480 min) - Metal concentration of Cd^{2+} and Pb^{2+}: (25–300 mg/L)	
12	Composite graphene oxide-framework membranes (MMM)	-	10 mg of GO	- Rejection rate of GO-IPDI membranes: methylene blue (MB): 97.6% rhodamine-B (RB): 96.2% methylene orange (MO): 96.9% congo red (CR): 98.24% - The rejection rate of GO-IPDI membranes: Cu^{2+}: 46.2% Pb^{2+}: 66.4% Cr^{3+}: 71.1% Cd^{2+}: 52.8% - Contact angle GO: 26 ° GO-IPDI: 53 °	- TMP: 1 bar - pH: 7 - Dyes feed solution: 10 mL with the concentration of 10 mg/L - Data was recorded every 5 min until it became steady	Zhang et al(b)., 2017

13	Cross-linked graphene oxide sheets via modified extracted cellulose (B)	- 0.2 g of GO powder	- Maximum adsorption capacity: Cu(II): 46.39 mg/g Pb(II): 186.48 mg/g	- pH: 7 (real water sample) - Flow rate: 10 mL/min (real water sample) - Pressure: 1 atm real water sample from 3 places.	Yakout et al., 2017
14	Graphene oxide (GO) impregnated mixed matrix membrane (MMM)	- 0.1, 0.2, 0.35 and 0.5 wt% of GO	- Adsorption capacity: Pb^{2+}: 79 mg/g Cu^{2+}: 75 mg/g Cd^{2+}: 68 mg/g Cr^{6+}: 154 mg/g - Regeneration: The membrane was regenerated in-situ, by acidic solution at pH 5.5 for one hour with flux recovery ratio over 0.9. - Contact Angle: 83° to 70°	- Feed concentration: 50 mg/l - TMP: 414 kPa - Cross flow rate: 40 L/h - pH:6.7,6.5 and 3.5	Mukherjee et al., 2016

			Natural Source			
15	Mesoporous-high surface area chitosan/poly(ethylene oxide) nanofibrous membrane (MMM)	- Chitosan (4 wt%) - PEO (3 wt%) - 80 wt% acetic acid solution	- Maximum adsorption capacity: Cu(II): 120 mg/g Zn(II): 117 mg/g Pb(II): 108 mg/g - S3 (60:40 chitosan:PEO ratio) possessed the maximum adsorption capability. - S3 is having the lowest contact angle, 27°.	- Time: 60 minutes	Shariful et al., 2017
16	Maize Leaves (B)		Removal Efficiency: - Pb (II): 85% - Cr(III): 56% - Cd(II): 50%	- pH: 5 - Agitation	Maximous et al.,2010
17	Rice Husk (B)		Removal Efficiency: - Pb (II): 93% - Cr(III): 58% - Cd(II): 66%	- pH: 5 - Agitation	Maximous et al.,2010

18	Chicken Eggshell (B)	-	Adsorbent dose of 1-7 g (7 g optimum)	-	The percentage adsorptions: Lead: 97% Copper: 95% Nickel: 94% Zinc: 80% - The equilibrium point for adsorption was attained within the first 120 min (Pb^{2+}: 98.33%) and 270 min (Zn^{2+}: 81.24%) of contact time. - Maximum percentage adsorption: Copper: 14.46% at 300 minutes Nickel: 3.47% at 360 minutes	- pH: 7 - Contact time: 360 min - Room temperature of 24 °C - Initial metal concentration: 100 ppm (Zn, Pb, Cu and Ni)	Mashangwa et al., 2017
19	Chicken Eggshell (B)	-	0.5 g of chicken eggshell - Concentration of Cu(II): 50 mg/L	-	Selective uptake of copper and affinity of adsorbent: 13.8995 L/g. - The adsorption occurred rapidly at the first 15 minutes and almost 100 % adsorption efficiency of Cu(II) was attained after 60 min.	- Initial concentrations of Cu(II) ions: 50 – 350 mg/L - pH: 4-8 - Time: 180 min - T= 30 °C	Aimi et al., 2013

20	Cellulose/alginic acid (RC-AC) ion exchange membrane (MMM)	- 6.4 wt% cellulose cuoxam - 3 wt% aqueous alginate solution	- The concentration extracted from the adsorbed membrane: Cd(II): 0.79 meq/g Sr(II): 0.75 meq/g - Time for establishing the ion exchange equilibrium: Cd(II): 30 minutes Sr(II): 90 minutes - Ions adsorbed on the RC-AC membrane were released in 2 mol/L HCI solution within 10 minutes.	- Initial concentrations: 100 mL of 200 mg/L Cd(II) ions and 150 mg/L Sr(II) ions - pH: 1-9 - Room temperature of 24 °C	Zhang et al., 1999
21	Cellulose acetate, nanochitosan, and polyethylene glycol blended ultrafiltration membrane (MMM)	- Cellulose acetate, nanochitosan, and polyethylene glycol of ratio 1:2:2	- Percentage removal of chromium: 68.436 % at 50 kPa and 95.640 % at 100 kPa for the duration of 5 minutes	- pH: 5, 7, and 9 - TMP: 50 and 100 kPa - Membrane thickness: 0.1 and 0.2 mm	Vinodhini and Sudha, 2016

Note: Adsorbents either in mixed matrix membrane (MMM) or bulk (B) are indicated above.

Besides heavy metal adsorption, Zr is also an effective adsorbent in fluoride removal. Fluoride is an essential element for both animals and human. It is also one of the contaminants in groundwater classified by the World Health Organization (WHO). The maximum acceptable concentration of fluoride is 1.5 mg/L (He et al., 2016). Excess intake of fluoride through drinks and food can cause diseases such as dental/skeletal fluorosis, neurotransmitters and fetal cerebral function (He et al., 2016). He et al. (2016) prepared zirconium metal-organic frameworks (Zr-MOFs) membrane. This metal-organic framework can achieve maximum adsorption capacity of 102.4 mg/g and highest percentage of 98% for the removal of fluoride under the operating conditions at pH 7 and initial fluoride concentration of 200 mg/L. It also showed this Zr-MOFs membrane was suitable for regeneration due to the maximum amounts of water that Zr-MOFs membrane can deal with were 2700, 2615, 2540, 2460, 2380 and 2235 mL, respectively after six adsorption-desorption cycles. This showed that Zr-MOFs membrane had only a slight decrease in the adsorption performance (He et al., 2016). Later, Zhang et al(a). (2017) also found excellent performance in the removal of fluoride by using the zirconium-chitosan/graphene oxide (Zr-CTS/GO) membrane. According to their findings, the removal efficiency of fluoride reached 88.47%. (9.54 to 1.10 mg/l) for the 50 mL groundwater sample with the dosage of 0.5 g Zr-CTS/GO under operating conditions of pH 7.39 for 60 minutes The adsorption mechanism for this Zr-CTS/GO membrane was Zr(IV) ions in metal complexes attracted fluoride ions with the displacement of –OH in Zr complexes by fluoride (Zhang et al(a)., 2017). In addition, the concentration of SO_4^{2-} dropped sharply from 99.70 to 2.74 mg/L (97.25% removal) while the concentration of bicarbonate, HCO_3- dropped sharply from 153.75 to 29.09 mg/l (81.08% removal) after adsorption. This showed that Zr-CTS/GO has an excellent selectivity for fluoride, bicarbonate and sulphate (Zhang et al(a)., 2017).

2.4.1.2 Zinc Oxide

Nano zinc oxide (ZnO) is an important inorganic functional material. The price of nano-ZnO is much lower than the other commonly used nano-adsorbents, such as TiO_2 and Al_2O_3 nanoparticles (Zhang et al., 2014). Based on Zhang et al. (2014) findings, the PVDF/ZnO hybrid membranes with the dosage of 3 wt% ZnO showed maximum adsorption capacity for Cu^{2+} (87.4 ug/cm^2) which was almost nine times higher than pristine PVDF films (9.83 ug/cm^2) at pH of 6, optimum equilibration time of 120 minutes and initial concentration of 20 mg/L of Cu^{2+}. Besides that, the contact angle

decreased with the increment of ZnO nanoparticles as shown in Figure 2.6, hence enhancing the surface hydrophilicity of membranes (Zhang et al., 2014). This showed that ZnO is a good option for the application in removal of heavy metal ions.

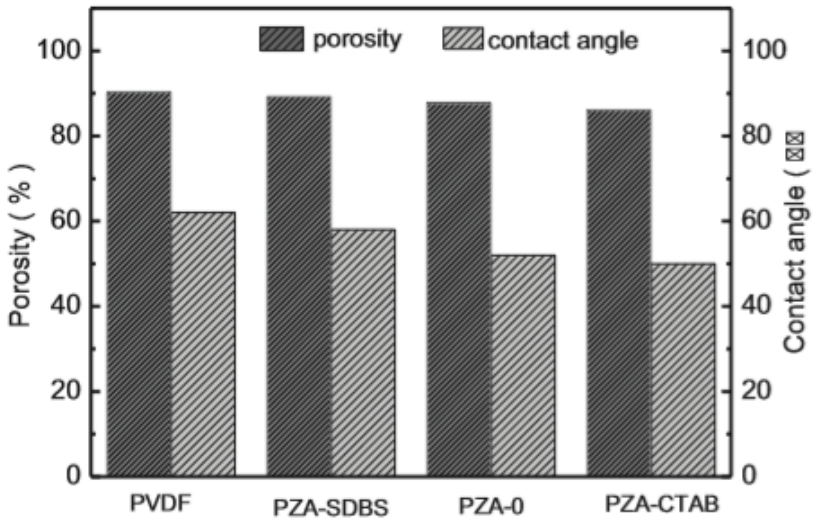

Figure 2.6: Comparison of Porosity and Contact Angle of PVDF and PVDF/ZnO Hybrid Membranes. (Zhang et al., 2014).

2.4.1.3 Iron and Iron Oxide

Koushkbaghi et al. (2017) prepared an aminated-Fe_3O_4 nanoparticles (0-4 wt%) filled chitosan/PVA/PES dual layers nanofibrous membrane. Based on the findings, the maximum adsorption capacities of Cr(VI) and Pb(II) ions were found to be quite similar (509.7 mg/g for Cr(VI) ions and 525.8 mg/g for Pb(II) ions), at optimum pH of 3 in a binary system. The reusability of the nanofibrous membrane in both adsorption and membrane ultrafiltration processes for 3 cycles showed the high capacity of synthesized nanofibrous membranes in the industry as a membrane or adsorbent as shown in Figure 2.7 (Koushkbaghi et al., 2017).

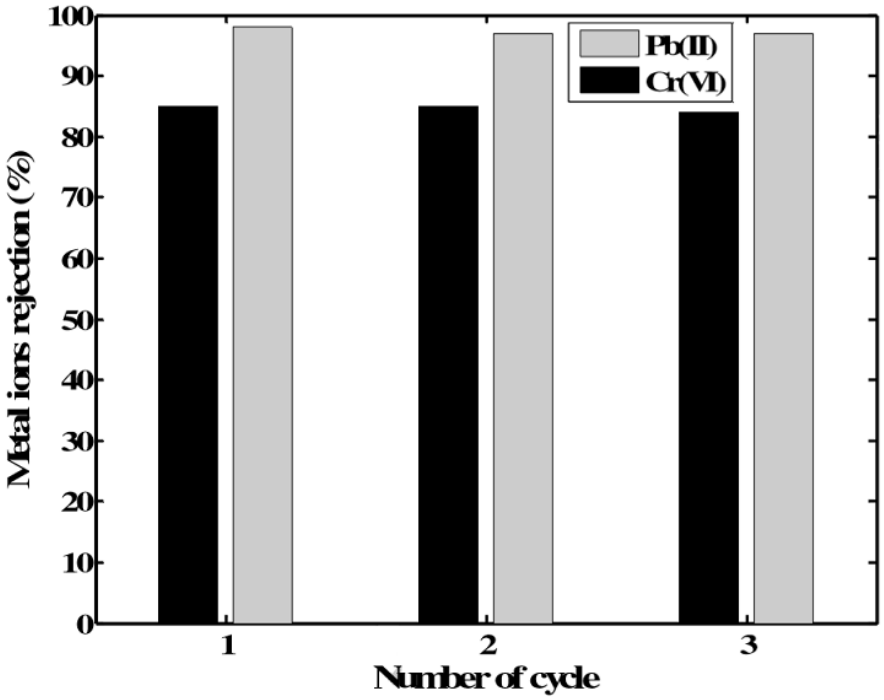

Figure 2.7: The Reusability of Nanofibrous Membrane in Both Adsorption and Membrane Processes for 3 Cycles. (Koushkbaghi et al., 2017).

Furthermore, Mondal et al. (2017) had prepared a nickel iron oxide nanoparticle incorporated hollow fiber mixed matrix membrane that consists of 3 wt% nanoparticle. This hollow fiber MMM had showed maximum adsorption capacity for lead (52 mg/g) followed by copper (42 mg/g), zinc (35 mg/g), cadmium (24 mg/g) nickel (17.5 mg/g) and chromium (18 mg/g) under the operating conditions of pH 7, feed heavy metal concentration 50 mg/L, cross-flow rate of 20 L/h and 69 kPa TMP in long duration run. Based on this findings, it showed more than 95% rejection of heavy metal and the membranes became more hydrophilic due to reduced contact angle from 77° to 64°. This MMM could be regenerated using 0.1 N HCl solution for 10 hours (Mondal, Dutta and De, 2017).

Besides, iron metal also can be used for phosphorus removal in preventing excessive amounts of phosphorus being discharged into water bodies, resulting in the occurrence of eutrophication and algal bloom. To prevent the happening of eutrophication, the phosphorus concentration in the discharging water must not exceed 0.1 mg P/L (Johir et al., 2016). Based on Park et al. (2017) findings, mixed metal oxide (Fe-Ti bimetal oxides) coated sulfonated polymer beads showed high selectively to phosphate ions (selectivity factor>25) against background ions (e.g., CI^-, NO^{3-}, and

SO_4^{2-}) and capable to achieve maximum adsorption capacity range of 7.14 mg-P/g to 59.0 mg-P/g metal with molar fraction of Ti to the total molar concentration of the two metals (i.e., Fe and Ti) varied from 0 to 6% under the operating conditions such as reaction time of 48 hours, 30 mL of synthetic feed water and at the temperature of 25℃. Through this findings, the Ca ion can play a role in bridging phosphate in the surface coordination in which it provides greater phosphorus binding than the direct coordination of phosphate. It also showed good recovery as approximately 97% of the phosphorus was recovered from the bead when 1.2 eq NaOH per L bed were added during the recovery process (Park et al., 2017).

2.4.2 Carbon Source

2.4.2.1 Graphene Oxide

Graphene oxide sheets (GO) have attracted the attention of researchers in the area of nanocomposites and material sciences due to its excellent electrical, physical and mechanical properties. GO has good dispersion in both organic solvents and water because it has a large surface area with a high number of functional groups such as OH, -COOH, -O- and C=O (Yakout et al., 2017). Recently, a number of studies have predicted that graphene with sub-nanometer pores can act as a highly selective and permeable filtration membrane due to their superior mechanical strength, thermal stability and chemical resistance (Zhang et al(b)., 2017).

Mukherjee et al. (2016) prepared the graphene oxide (GO) impregnated MMM with the dosage of GO at 0.1, 0.2, 0.35 and 0.5 wt%. Based on the findings, high adsorption capacity was observed for Pb^{2+} (79 mg/g), Cu^{2+}(75 mg/g), Cd^{2+}(68 mg/g) and Cr^{6+}(154 mg/g) at natural pH, 6.7, 6.5, 6.4 and 3.5, respectively under the operating conditions of 50 mg/L feed concentration, TMP of 414 kPa and 40 L/h of cross-flow rate. The contact angle reduced from 83° to 70°, implied an increase in membrane hydrophilicity. The MMM was regenerated in-situ, by a wash with an acidic solution at pH 5.5 for one hour. The high flux recovery ratio over 0.9 showed that the MMM has high flux recover in the adsorption and desorption process (Mukherjee et al., 2016).

Based on Zhang et al(b). (2017) findings, with the dosage of 10 mg of graphene oxide, the rejection rate of graphene oxide/isophorone diisocyanate (GO-IPDI) membranes for methylene blue (MB), rhodamine-B (RB), methylene orange (MO) and

congo red (CR) was 97.6%, 96.2%, 96.9% and 98.24%, respectively. The rejection rate of GO-IPDI membranes for Cu^{2+}, Pb^{2+}, Cr^{3+} and Cd^{2+} were 46.2%, 66.4%, 71.1% and 52.8%, respectively under the operating conditions of 1 bar, pH 7 and 10 mL of the dyes feed solution with the concentration of 10 mg/L. The contact angle of the GO and GO-IPDI membranes were 26 ° and 53 °, respectively. This illustrated the hydrophilic functional groups decreased and GO-IPDI membrane has a lower rejection rate compared with GO membrane as shown in Figure 2.8 (Zhang et al.(b), 2017). According to Zhang et al.(b) (2017), the performance degradation might due to the smaller size of heavy metal ions compared with the interlayer distance of the GO-IPDI. Hence, it limited the physical sieving effect for the metal ion rejection. Besides that, the oxygen functional groups on the surface of graphene oxide might have been consumed after the introduction of IPDI. Observable gaps can be observed because of the weak interaction between the GO layers when the GO membrane was not modified with IPDI. The surface was complete and undamaged when IPDI was introduced to GO layers to form GO-IPDI membrane. This indicates that GO-IPDI good to be used in the application of heavy metal removal due to its excellent stability of GO-IPDI membrane. The stability was attributed to the formation of strong chemical bonds between GO nanosheets supported by IPDI linkers, which was helpful to prevent the membranes peeling off from PVDF surface (Zhang et al(b)., 2017).

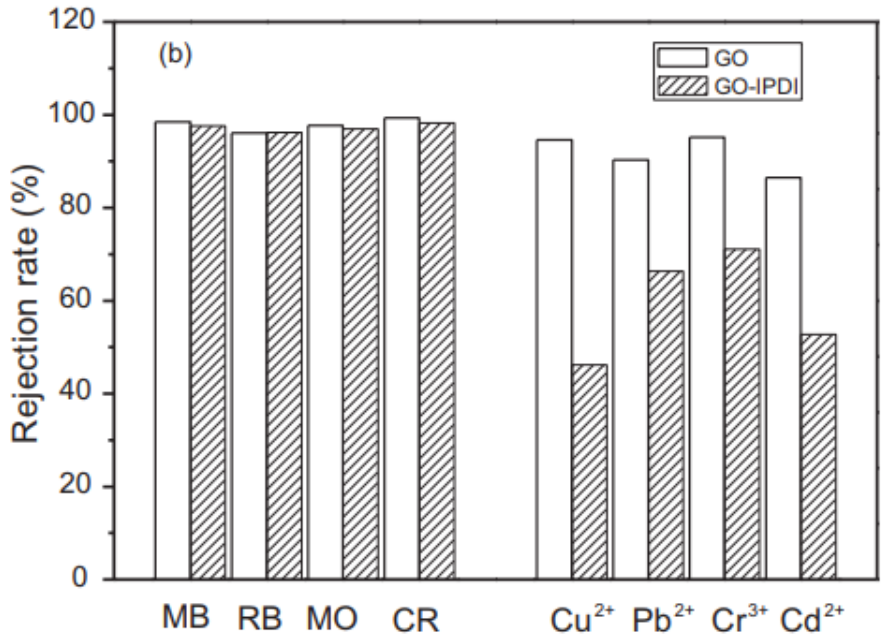

Figure 2.8: Rejection Rate of the Heavy Metal Ions (Cu^{2+}, Pb^{2+}, Cr^{3+} and Cd^{2+}) and Dyes for Pure GO Membrane and GO-IPDI Membrane. (Zhang et al(b)., 2017)

According to the findings of Yakout et al. (2017), cross-linked graphene oxide sheets via modified extracted cellulose with the dosage of 0.2 g of GO powder capable to achieve maximum adsorption capacity of 46.39 and 186.48 mg/g for Cu(II) and Pb(II), respectively under the operating conditions of pH 7, pressure of 1 atm and flow rate of 10 mL/min in the real water sample (drinking tap water, sea water sample from Mediterranean Sea water at Alexandria, Egypt and industrial wastewater sample from Al-Nubariya canal.)

2.4.2.2 Carbon Nanotube

Ainscough et al. (2017) developed a hybrid super hydrophilic ceramic membrane by incorporating carbon nanotube (CNT). The membrane had average adsorption capacities of 99.39% for cadmium, 99.61% for mercury, 99.70% for nickel, 99.72% for cobalt, and 99.97% for lead. Post experiment treatment included 2 wt% sodium hydroxide washing at 50 ℃ for 1 h followed by a 1% citric acid. The former was aimed to remove organic foulant while the latter was used to remove inorganic foulant. In this study, the membrane flux recovery was only 12% of the original pre-experimental specific clean water flux (Ainscough et al., 2017). Ainscough et al. (2017) concluded that the used motor oil as wastewater sample had caused irreversible fouling of the membrane due to the internal pore and surface blocking as clear staining of the membrane was visible on both the outside and inside surfaces.

2.4.2.3 Activated Carbon

Maximous et al. (2010) had also performed the research on the activated carbon by using the operating conditions such as pH of 5 and it showed that activated carbon can achieve 98% Pb (II) removal efficiency, 95% Cr(III) removal efficiency and 83% Cd(II) removal efficiency.

Al-Malack and Basaleh (2016) investigated the removal of Cd^{2+} and Pb^{2+} ions by using activated carbon produced from municipal organic solid waste. Through this finding, the results showed that optimum adsorption of Cd^{2+} and Pb^{2+} ions were obtained at pH of 5, metal concentration of 100 mg/L, contact time of 180 min and an adsorbent dose of 200 mg per 50 mL of metal solution. Besides that, the isotherms showed that the maximum adsorption capacity of Cd^{2+} and Pb^{2+} ions were 61 and 90 mg/g, respectively, at pH value of 5 and equilibrium time of 120 min (Al-Malack and Basaleh, 2016).

2.4.3 Natural Source

2.4.3.1 Chicken Eggshells

Chicken eggshell has been used as an adsorbent to remove heavy metal ions such as lead, nickel, copper and zinc ions (Aimi et al., 2013; Mashangwa et al., 2017). Chicken eggshell can be used to adsorb heavy metal in wastewater due to its high calcium carbonate content. The mechanism of adsorption is played by carbonate groups on the chicken eggshells that have cation-exchange properties with the heavy metal ions (Aimi et al., 2013). In addition, the porosity of eggshell had made it as an attractive material to be used as an adsorbent. The eggshell characteristically consists of ceramic material, namely, the cuticle on the outer surface, a spongy layer, and an inner lamellar (or mammillary) layer, arranged in a three-layered structure. More than 90 % of the material in the eggshell is represented by the mammillary and spongy layers that form a matrix composed of protein fibres bonded to calcite (calcium carbonate). The eggshell is an efficient adsorbent due to the two layers are fashioned in such a way that there are many circular pores (Aimi et al., 2013).

Aimi et al. (2013) had prepared chicken eggshells with the dosage of 0.5 g of chicken eggshell for the removal of 50 mg/L concentration of Cu(II) ions. Based on Aimi et al. (2013) findings, the selective uptake of copper and affinity of adsorbent was 13.8995 L/g and the adsorption occurred rapidly at the first 15 minutes and almost 100% adsorption efficiency of Cu(II) was attained after 60 min under the operating conditions such as pH of 4 to 8, contact time of 180 minutes, temperature of 30 °C, and initial concentrations of Cu(II) ions in the range of 50 – 350 mg/L. In this findings also, pH 7 had been found to be the optimum pH and the optimum agitation rate was determined at 350 rpm.

Later, Mashangwa et al. (2017) also showed that chicken eggshells had a high potential for the use as an effective and low-cost adsorbent for the removal of Pb^{2+}, Cu^{2+}, Ni^{2+}, and Zn^{2+}. The percentage adsorptions were 97% for lead, 95% for copper, 94% for nickel, and 80% for zinc from the standard aqueous solutions with the dosage of 7 g of adsorbent under the operating conditions of pH 7, optimum contact time of 360 min, room temperature of 24 °C and initial metal concentration of 100 ppm (Zn, Pb, Cu and Ni). The research team also reported that the equilibrium point for adsorption attained within the first 120 min for Pb^{2+} (98.33%) and 270 min for Zn^{2+}

(81.24%) of contact time. copper and nickel, on the other hand, showed a maximum percentage adsorption of 14.46% and 3.47% at 300 and 360 min, respectively.

2.4.3.2 Others Adsorbents

Chitosan, one kind of polysaccharides is under study in the application for the removal of heavy metal ions in these recent years due to its availability in nature and special properties like non-toxicity, biocompatibility, biodegradability and metal ion chelation (Shariful et al., 2017). Shariful et al. (2017) developed a mesoporous-high surface area chitosan/poly(ethylene oxide) (PEO) nanofibrous membrane with 4 wt% of chitosan, 3 wt% of PEO and 80 wt% acetic acid solutions for heavy metal ions removal. Two polymer solution were mixed at different chitosan/PEO weight ratios (40:60-S1, 50:50-S2, 60:40-S3, 70:30-S4, and 80:20-S5) and it was found that the S3 membrane (60:40 chitosan:PEO ratio) possessed the maximum adsorption capability. The maximum adsorption capacity for S3 for Cu(II), Zn(II) and Pb(II) ions were 120, 117 and 108 mg/g, respectively with the operating time of 60 minutes. Besides that, S3 also showed good hydrophilic property when S3 is having the lowest contact angle which is 27° among the others (Shariful et al., 2017). Moreover, Vinodhini and Sudha, (2016) had shown that the cellulose acetate, nanochitosan, and polyethylene glycol blended ultrafiltration membrane of ratio 1:2:2 can achieve 68.436% and 95.640% removal efficiency of chromium at 50 kPa and 100 kPa, respectively for the duration of 5 minutes at pH 7 using 0.2 mm thickness of membrane.

Maximous et al. (2010) had proven that maize leaves and rice husk can be good alternative choices for heavy metal ions removal. In Maximous et al. (2010) findings, maize leaves can achieve 85% Pb (II) removal efficiency, 56% Cr(III) removal efficiency and 50% Cd(II) removal efficiency whereas rice husk can achieve 93% Pb (II) removal efficiency, 58% Cr(III) removal efficiency and 66% Cd(II) removal efficiency. For the removal of Pb (II), rice husk had shown better removal efficiency which is 8% more than maize leaves. For the removal of Cr(III), the removal efficiencies for both rice husk and maize leaves were almost similar to each other because there was only 2% in different. For the removal of Cd(II), the rice husk performed better where the removal efficiency was 16% more than the maize leaves. Compared with the Al_2O_3/PES and ZrO_2/PES, the rice husk and maize leaves showed lower removal efficiencies of Pb(II) and Cr(III) ions. (10.46% lower for Pb(II) ions, 33.72% lower for Cr(III) ions) However, the rice husk and maize leaves showed better

removal efficiencies of Cd(II) (79.14% higher) compared with Al_2O_3/PES and ZrO_2/PES (Maximous et al., 2010).

The effective use of cellulose and alginate not just only conserve the limited petroleum resources; it also protects the environment for their biodegradability. In addition, it has been reported that the inhibition of the alginate on the toxicity of cadmium and also the radioactive of strontium (Zhang et al., 1999). Zhang et al. (1999) had prepared a cellulose/alginic acid (RC-AC) ion exchange membrane with the dosage of 6.4 wt% cellulose cuoxam and 3 wt% aqueous alginate solution. Based on Zhang et al. (1999) findings, the concentrations extracted from the adsorbed membrane for both Cd(II) and Sr(II) are 0.79 and 0.75 meq/g, respectively under the operating conditions of pH 1-9, room temperature of 24 °C and initial concentrations of 100 mL of 200 mg/L Cd(II) and 150 mg/L Sr(II). The time for establishing the ion exchange equilibrium for both Cd(II) and Sr(II) are 30 minutes and 90 minutes, respectively and the ions adsorbed on the RC-AC membrane were released in 2 mol/L HCI solution within 10 minutes (Zhang et al., 1999).

CHAPTER 3

METHODOLOGY

3.1 General Preview

Fabrication of the zinc oxide/graphene oxide polysulfone mixed matrix membrane (ZnO/GO PSF MMMs) to remove heavy metal ions was described in this chapter. The materials, membrane fabrication technique, membrane characterization methods, various adsorption conditions, adsorption models and desorption and regeneration of the membrane were included.

3.2 Materials

The membranes were made from polysulfone (PSF) (Udel® P-1700) with a nominal size of 2 mm, supplied by Solvay. N-methyl-2-pyrrolidone (NMP) was used as a solvent to dissolve the polymer and the specification was EMPLURA® 1-Methly-2-Pyrrolidone originated by Merck. Zinc oxide/graphene oxide nano-powder (ZnO/GO) were used as the nano-adsorbent. Cd^{2+} stock solutions were prepared by dissolving cadmium chloride anhydrous, $CdCl_2$ (Sigma Aldrich) in deionized water. 37 wt% hydrochloric acid (EMSURE® by Merck) and sodium hydroxide pellets (R&M Chemicals) were used for adjusting the pH of the Cd^{2+} solution.

3.3 Preparation of ZnO/GO PSF MMM

3.3.1 Casting Solution Preparation

Before the preparation of the casting solution, PSF was placed into a 250 mL of beaker and it was dried in a drying oven at 60 °C overnight to remove the moisture content (Figure 3.1). The PSF, NMP, ZnO/GO composites used were 20 wt%, 79.8 wt% and 0.2 wt% (1 wt% based on PSF), respectively. The preparation of ZnO/GO composites is not under the scope of this study and was described elsewhere (Chong et al., 2017).

Firstly, 39.9 mL of NMP was poured into a 100 mL of beaker and it was heated to 60 °C with the hot plate. In the same time, it was stirred with a magnetic stirrer at a rate of 500 rpm. Then, 20 g of PSF was added into the heated NMP solution with a spatula and the beaker was sealed with paraffin film (Figure 3.2). The beaker was then left undisturbed for 6 hours. After 6 hours, the heating and stirring processes were

stopped. (0.1 g)1 wt% of ZnO/GO composites were added into the casting solution and the solution was then sonicated for 30 minutes by using the ultrasonic bath to disperse the ZnO/GO (Figure 3.3). The casting solution was left undisturbed overnight to remove the entrapped air bubbles and it was sealed properly to prevent the solidification of the solution. The prepared casting solution will be in black colour due to the presence of ZnO/GO (Figure 3.4).

Figure 3.1: Drying Oven

Figure 3.2: Casting Solution

Figure 3.3: Sonication of Casting Solution

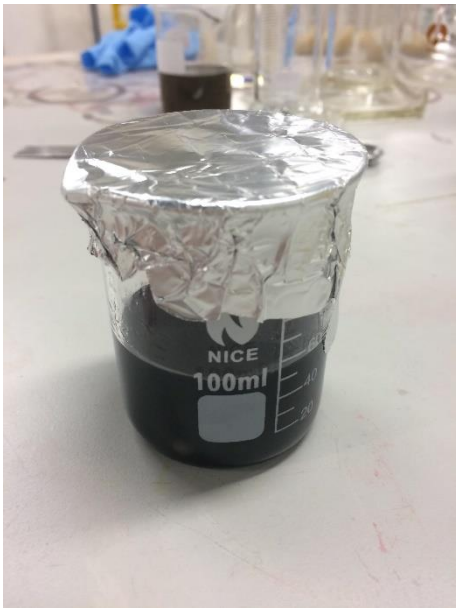

Figure 3.4: Prepared Casting Solution

3.3.2 Membrane Casting

After preparing the casting solution, the membranes were cast on a flat glass plate by using a casting blade that has been adjusted to the thickness of 200 µm. The film together with the glass plate were immersed in a 5 L of distilled water for the process of phase inversion. The membranes were then transferred to another water bath containing distilled water after 30 minutes. The membranes were left undisturbed for 24 hours for complete phase inversion process.

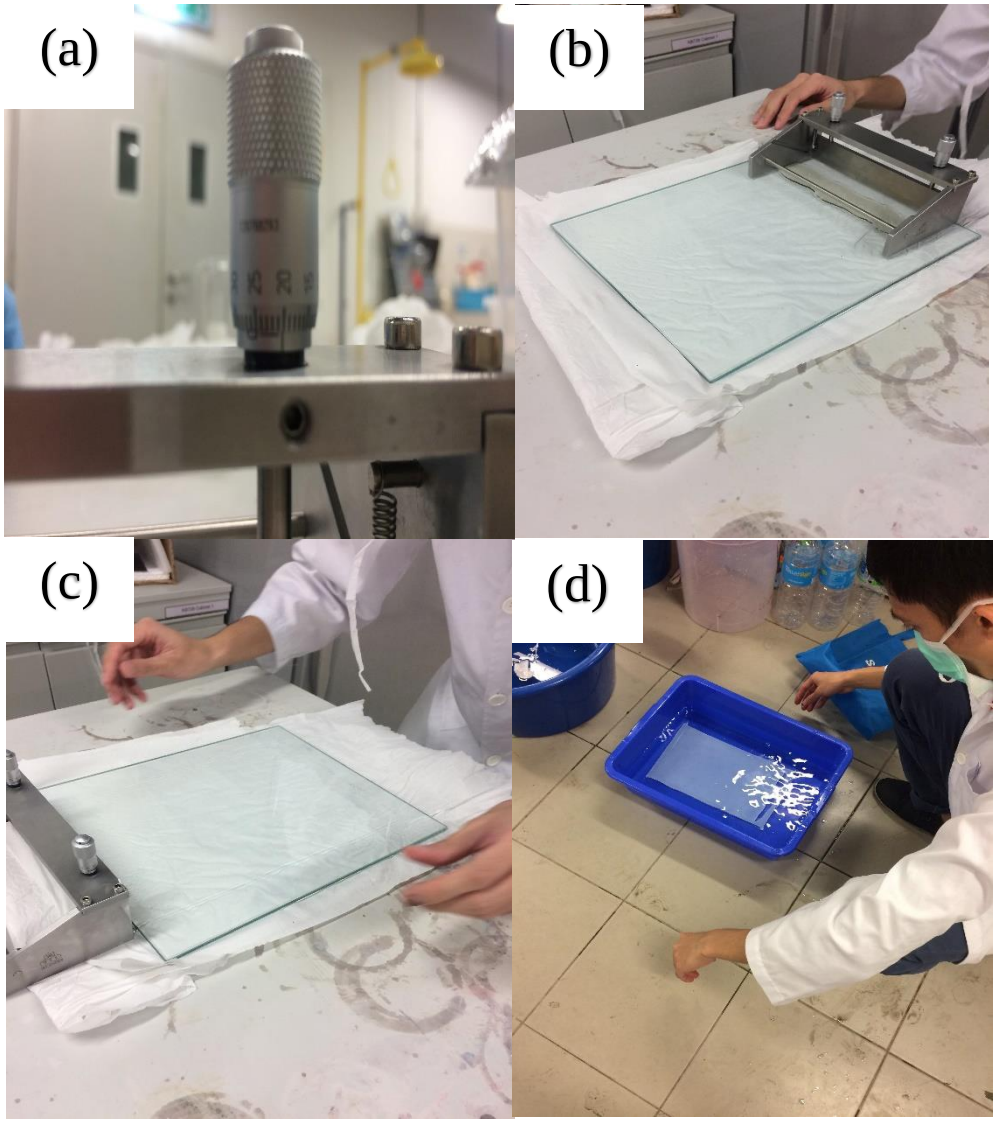

Figure 3.5: Membrane Casting Procedure; (a) Blade's scale adjustment (b) Prepared casting solution was poured onto the glass plate (c) Membrane casting by using the blade (d) Phase inversion process in water bath

3.4 Membrane Characterization

3.4.1 Membrane Morphology (SEM)

Scanning electron microscopy (SEM) was used to observe the cross-section area and surface morphologies of neat PSF and ZnO/GO PSF MMMs before and after the adsorption process. By using the liquid nitrogen cracking method, the membrane samples were cracked before the SEM analysis. The thickness of each of the membranes was measured during the image analysis. Moreover, the images of each membrane were taken at the magnification of 2000x. The equipment SEM (Hitachi S-3400N) used in this research is shown in Figure 3.6.

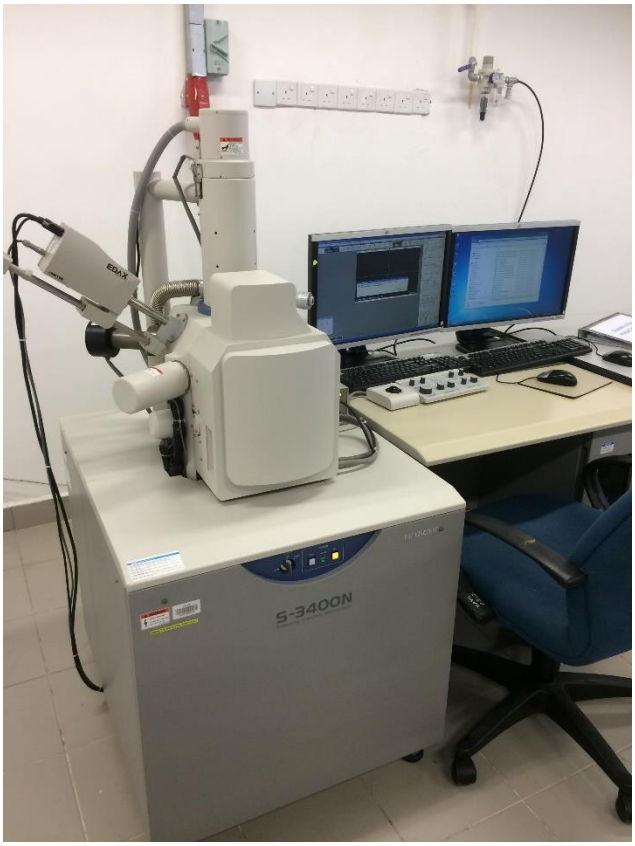

Figure 3.6: SEM Analysis

3.4.2 Elemental Analysis (EDX)

Energy Dispersive X-ray spectroscopy (EDX) was used to identify the elements (ZnO and Cd^{2+}) and also their composition in the membrane. Energy Dispersive X-ray spectroscopy (EDX) is a technique that has been used together with scanning electron microscopy (SEM). During the bombardment by an electron beam to characterize the

elemental composition of the analysed volume, the EDX technique detects X-rays that have been emitted from the sample (Mee-inc.com, 2018). In this study, samples that have been selected were neat PSF membrane and ZnO/GO PSF MMMs with 1 wt% ZnO/GO loadings before and after the process of adsorption.

3.4.3 Adsorbed Species Analysis (FTIR)

Fourier-tansform Infrared spectroscopy also known as FTIR Analysis or FTIR Spectroscopy is an analytical technique used to identify polymeric, organic and inorganic materials (Rtilab.com, 2018). The FTIR instrument delivers infrared radiation of about 10,000 to 100 cm^{-1} through a sample, with some radiation absorbed and some passed through. The absorbed radiation is converted into vibrational or rotational energy by the molecules. The resulting signal at the detector presents as a spectrum, typically from 4000 cm^{-1} to 400 cm^{-1} and it represents the molecular fingerprint of the sample. Each chemical structure will produce a special spectral fingerprint and it makes FTIR analysis a powerful tool for chemical identification (Rtilab.com, 2018). The equipment FTIR (Nicolet iS10) used in this research is shown in Figure 3.7.

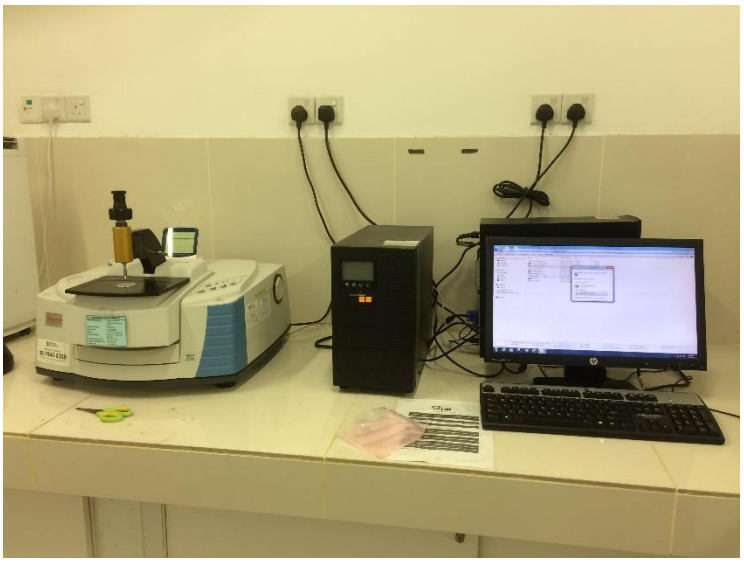

Figure 3.7: FTIR Analysis

3.5 Stock Solution Preparation

100 ppm of the Cd^{2+} solution was prepared by dissolving 163.09 mg of $CdCl_2$ in deionized water in a 1 L volumetric flask. The mass of $CdCl_2$ required was calculated with Equation 3.1. A sample calculation is shown in Appendix A.

$$mass\ of\ \mathrm{Cd}Cl_2 = V \text{ x } \frac{MW\ of\ \mathrm{Cd}Cl_2 \text{ x ppm of } Cd^{2+}}{MW\ of\ Cd^{2+}} \text{ x } stoichiometry \qquad (3.1)$$

where,

V = volume of the stock solution, L

$MW\ of\ CdCl_2$ = molecular weight of $\mathrm{Cd}Cl_2$, (g/mol)

$MW\ of\ Cd^{2+}$ = molecular weight of Cd^{2+}, (g/mol)

stoichiometry = stoichiometry in $CdCl_2$

3.6 Preparation of Different Concentration of Cd^{2+} Solutions

Different concentration of Cd^{2+} (5 ppm, 10 ppm, 15 ppm, 20 ppm and 25 ppm) solutions were prepared by diluting the 100 ppm of Cd^{2+} stock solution using the dilution factor equation as shown in Equation 3.2. A sample calculation is shown in Appendix B.

$$C_1V_1 = C_2V_2 \qquad (3.2)$$

where,

C_1 = concentration of Cd^{2+} stock solution, ppm

C_2 = desired concentration of Cd^{2+} stock solution, ppm

V_1 = volume of Cd^{2+} stock solution required for dilution, mL

V_2 = desired volume of Cd^{2+} stock solution, mL

A Cd^{2+} calibration curve was prepared by using the different concentration of Cd^{2+} (0 ppm, 5 ppm, 10 ppm, 15 ppm, 20 ppm and 25 ppm) solutions, analysed by the instrument ICP-OES. The calibration curve is illustrated in Appendix C. The R-squared obtained is 0.9999 and this shows that the calibration curve is accurate and the results obtained is reliable.

3.7 Heavy Metal Adsorption Performance Test

Seven cm^2 (1 cm x 7 cm) of each membrane was put into 10 mL of Cd^{2+} solutions under various conditions for the determination of static uptake capacity of Cd^{2+} on ZnO/GO PSF MMMs. The initial and final concentration of Cd^{2+} were measured by using the ICP-OES (Perkin Elmer Optima 7000 DV) (Figure 3.8). Before proceeding to the ICP-OES test, the tubes were sent to a vortex mixer to ensure the solutions are in the homogenous state (Figure 3.9). The static adsorption capacity can be obtained by using the Equation 3.3 (Khan et al., 2013).

$$q_e = \frac{(C_o - C_e)V}{m} \tag{3.3}$$

where,

q_e = adsorption capacity, mg/cm^2

C_o = initial concentration of metal ions in solution, mg/L

C_e = equilibrium concentration of metal ions in solution, mg/L

V = volume of the solution, L

m = area of membrane, cm^2

Figure 3.8: ICP-OES Analysis

Figure 3.9: Vortex Mixer

3.7.1 Effect of pH Conditions on Adsorption Performance

By titrating 0.1 M of hydrochloric acid and 0.1 M of sodium hydroxide solutions into the Cd^{2+} solution, the pH values of the Cd^{2+} solution can be changed. Sample calculations for the preparation of 0.1 M of hydrochloric acid and 0.1 M of sodium hydroxide solutions are shown in Appendix D and E. The hydrochloric acid solution can be used to reduce the pH values of the Cd^{2+} solution whereas the sodium hydroxide solution can be used to increase the pH values of the Cd^{2+} solution. The pH values of the Cd^{2+} solutions were adjusted to pH of 2.3, 3.5, 5.5, 8.3, 10 and 11. Then, 10 mL of the solutions with different pH values were put into a 15 mL centrifuge tube. Five pieces of the membranes with the area of (1 cm x 7 cm) were cut and placed into each tube. The tubes were left undisturbed for 3 hours. The membranes were taken out from the solutions after 3 hours. All the solutions must be filtered properly by using the filter papers before proceeding to the ICP-OES test as the precipitate of Cd^{2+} will cause damages to the instrument. Figure 3.10 shows the static adsorption setup for different pH values on adsorption performance.

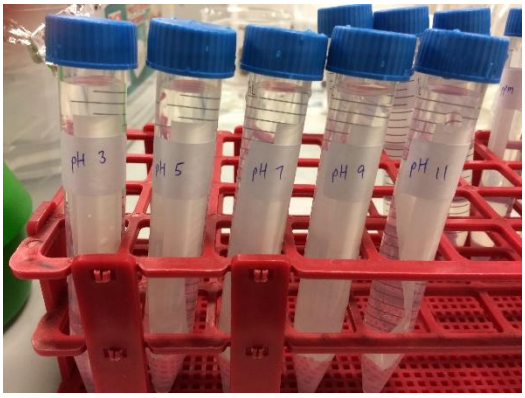

Figure 3.10: Static Adsorption Setup for Different pH Values

3.7.2 Effect of Contact Time on Adsorption Performance

To understand how the contact time affects the adsorption performance, four pieces of the membranes with the area of (1 cm x 7 cm) were cut and placed into the 15 mL centrifuge tubes that contain 10 mL of 25 ppm Cd^{2+} solution. The membranes were then taken out from the tubes after the time of 1, 2, 3 and 4 hours, respectively and the tubes were sent for analysis using the ICP-OES.

3.7.3 Effect of Initial Concentration of Cd^{2+} on Adsorption Performance

To investigate how the effect of initial concentration of Cd^{2+} on adsorption performance, five pieces of the membranes with the area of (1 cm x 7 cm) were cut and placed into the 15 mL centrifuge tubes that contain 5, 10, 15, 20 and 25 ppm of Cd^{2+} solution, respectively. Each of the tubes contains 10 mL of Cd^{2+} solution with a different initial concentration of Cd^{2+}. The membranes were then taken out from the tubes after the time of 3 hours to ensure the equilibrium adsorption capacity can be achieved. The tubes were then sent to the ICP-OES to measure the concentration of Cd^{2+} in the solution.

3.7.4 Effect of Number of Membranes on Adsorption Performance

To study how the effect of the number of membranes on adsorption performance, six 15 mL centrifuge tubes with 10 mL of Cd^{2+} solution were filled with 0, 1, 2, 3, 4 and 5 membranes, respectively. Each membrane has the area of (1 cm x 7 cm) and the membranes were then taken out from the tubes after the time of 5 hours to ensure the equilibrium adsorption capacity can be achieved. The tubes were then sent to the ICP-OES to measure the concentration of Cd^{2+} in the solution.

3.7.5 Effect of Humic Acid on Adsorption Performance

To prepare the humic acid solution, 0.05 g of powder humic acid was dissolved in a 40 mL of 0.1 M NaOH solution. To understand how the humic acid affects the adsorption performance, two pieces of the membranes with the area of (1 cm x 7 cm) were cut and placed into the 15 mL centrifuge tubes that contain 10 mL of Cd^{2+} solution with the concentration of 25 ppm and 4 mL of humic acid solution, respectively. The membranes were then taken out from the tubes after the time of 5 hours to ensure the equilibrium adsorption capacity can be achieved. The tubes were then sent to the ICP-OES to measure the concentration of Cd^{2+} in the solution.

3.8 Adsorption Isotherm

Langmuir and Freundlich adsorption isotherms were used to describe the adsorption isotherm of experimental data. Langmuir equation assumes that a monolayer adsorption onto a fully homogeneous surface with a negligible interaction between the adsorbed molecules and a finite number of identical sites (Khan et al., 2013). However, the Freundlich model does not predict surface saturation and it considers the existence of a multilayered structure (Barkhordar and Ghiasseddin, 2004). Equation 3.4 and 3.5 show the linearized Langmuir's equation and the linearized Freundlich's equation, respectively.

$$\frac{C_e}{q_{eq}} = \frac{1}{b \cdot q_{max}} + \frac{1}{q_{max}} C_e \tag{3.4}$$

where,

q_{eq} = equilibrium adsorption capacity, mg/cm^2

Ce = equilibrium concentration of metal ions, mg/L

q_{max} = maximum adsorption capacity, mg/cm^2

b = Langmuir constants of adsorption, L/mg

$$\log q_e = \log K_f + \frac{1}{n}\log C_e \quad (3.5)$$

where,

q_{eq} = equilibrium adsorption capacity, mg/cm^2

Ce = equilibrium concentration of metal ions, mg/L

K_f = sorption capacity constant (L/g)

n = sorption intensity constant

Graphs of C_e/ q_{eq} against C_e and log q_e against log C_e were plotted with the data obtained from section 3.7.3 (Yakout et al., 2017).

3.9 Adsorption Kinetics

For a better understanding of the adsorption process, the kinetic models such as linear pseudo-first order and linear pseudo-second order were employed as shown in Equation 3.6 and 3.7, respectively (Fang et al., 2017). If the kinetic model best fits the linear pseudo first order, it implies that the reaction is more favour towards physisorption. However, it assumes that chemisorption is the rate determining step if the kinetic model best fits the linear pseudo-second order (Fang et al., 2017).

Chemisorption is the process of adsorption in which the forces involved are valance forces whereas physisorption is the process of adsorption in which the forces involved are intermolecular forces such as van der Waals forces (Old.iupac.org, 2018).

$$\ln (q_{eq} - q_t) = \ln (q_{eq}) - k_1 t \quad (3.6)$$

$$\frac{t}{q_t} = \frac{1}{k_2 \cdot q_{eq}^2} + \frac{1}{q_{eq}} t \quad (3.7)$$

where,

q_{eq} = equilibrium adsorption capacity, mg/cm^2

q_t = adsorption capacity at time t, mg/cm^2

k_1 = rate constant for pseudo first order, 1/h

t = time, h

k_2 = rate constant for pseudo second order, cm^2/mg.h

Graphs of $\ln(q_{eq} - q_t)$ against t and t/ q_t against t were plotted by using data obtained from section 3.7.2.

3.10 Desorption and Regeneration

An ideal adsorbent must not only show higher adsorption capability, but it should also show good desorption performance because it would maintain the adsorption efficiency in long term and eventually reduce the operation cost. Hence, desorption and regeneration are very significant for the application of the MMMs in heavy metal adsorption (Peng et al., 2017). It was reported by Mukherjee et al. (2016) that GO with adsorbed heavy metal molecules can be regenerated in an acidic solution.

Firstly, the membrane that has been used for the adsorption of Cd^{2+} in 10 mL Cd^{2+} solutions with 25 ppm was washed thoroughly with distilled water for 15 minutes. Then, the membrane was put into an acidic solution, HCl (0.1 M) and it was stirred with a magnetic stirrer at a rate of 500 rpm for 45 minutes. Later, the membrane was taken out and rinsed with distilled water until the pH of water becomes neutral. The membrane was then put back into the 10 mL Cd^{2+} solutions with 25 ppm for the application of adsorption of Cd^{2+} again. The maximum adsorption capacity was then determined. Three cycles of desorption and regeneration were applied to investigate the desorption performance of the membrane. 10 mL of the used HCI (0.1 M) was put into the centrifuge tubes and the tubes were then sent to ICP-OES to measure the concentration of Cd^{2+} in the HCI solution.

3.11 Bulk Analysis

In order to study the adsorption performance of the ZnO/GO in both MMMs and bulk, a bulk analysis was being conducted. 0.13 g of ZnO/GO was put directly into a 50 mL of Cd^{2+} solution with the concentration of 100 ppm. The solution was filtered after 6 hours to ensure the equilibrium adsorption capacity can be achieved and 10 mL of the filtered solution was put into a 15 mL centrifuge tube. The tube was then sent to the ICP-OES to measure the concentration of Cd^{2+} in the solution. Figure 3.11 shows the bulk analysis setup.

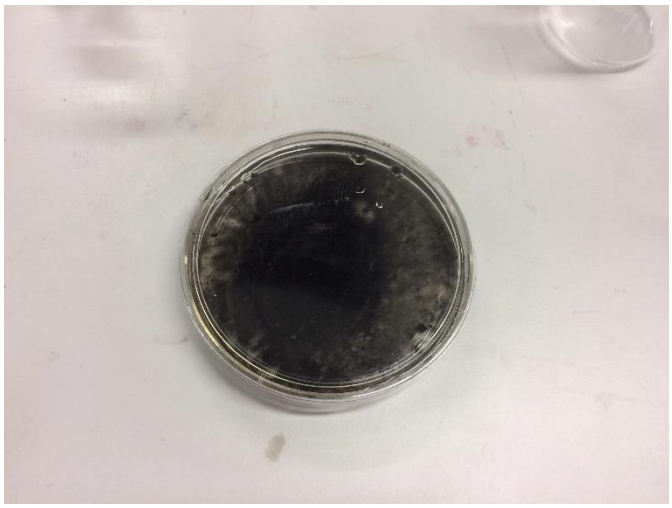

Figure 3.11: Bulk Analysis Setup

CHAPTER 4

RESULTS AND DISCUSSIONS

4.1 Membrane Characterization

4.1.1 Scanning Electron Microscopy (SEM)

The scanning electron microscope (SEM) is a very useful tool to characterize the surface morphology of the membrane (Vinodhini and Sudha, 2016). The surface morphology of the neat PSF and 1 wt% ZnO/GO PSF MMM were observed using SEM and are shown in Figure 4.1. Figure 4.1 (a) and (b) show the cross-sectional SEM images of neat PSF membrane and 1 wt% ZnO/GO PSF MMM, respectively. As shown in Figure 4.1, the short asymmetric finger like pore structures were formed at the upper layer and followed by porous sub-layer contained macro-voids at the bottom layer. This shows that a slow solvent and non-solvent exchange rate during the process of phase inversion (Chong et al., 2017). Based on Figure 4.1, the membrane shows appreciable differences between the neat PSF membrane and 1 wt% ZnO/GO PSF MMM. The pore size for the ZnO/GO PSF MMM is larger than the neat PSF membrane. This is because the oxygen functional groups of the ZnO/GO had attracted the non-solvent towards the polymer solution resulting in an enhanced inflow of non-solvent and outflow of solvent. Therefore, the phase inversion process was accelerated (Chong et al., 2017).

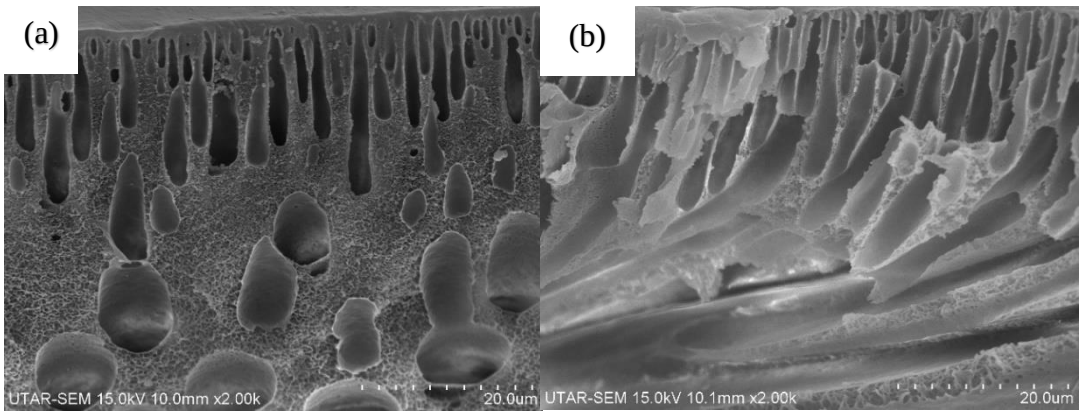

Figure 4.1: SEM Images at Magnification of 2000x (a) Neat PSF (b) 1wt% ZnO/GO PSF MMM

4.1.2 Elemental Analysis (EDX)

Table 4.1 presented the elemental analysis result for the neat PSF membrane (0 wt% ZnO/GO), 1 wt% ZnO/GO PSF MMMs before and after adsorption of Cd^{2+}. It is noted that carbon (C), oxygen (O) and sulphur (S) are the dominant elements of polysulfone (PSF) polymer. Moreover, there are approximately 1.16 wt% of Zn being detected before the adsorption process which indicated the presence of ZnO nanoparticles in the membranes. There are also 0.26 wt% of Cd element being detected in the 1 wt% ZnO/GO PSF MMM after the adsorption of Cd^{2+}, this shows that Cd^{2+} had been adsorbed on the surface of the MMM by ion exchange reaction between heavy metal ions and the proton on -COOH or -OH oxygenous functional groups for both the GO and ZnO. The 1 wt% ZnO/GO MMM that was used for EDX elemental analysis undergone the operation conditions of pH 5.5, the initial Cd^{2+} concentration of 25 ppm and contact time of 3 hours.

Based on Zhang et al(a). (2017) findings, the presence of Zr element in zirconium-chitosan/graphene oxide (Zr-CTS/GO) membrane was confirmed by using energy dispersive spectrometer (EDS) which refers to the same measurement as energy dispersive X-ray spectroscopy (EDX) with an atom percentage of 2.97%. It was indicated that Zr(IV) was wrapped within CTS and GO complex.

Table 4.1: EDX Elemental Analysis Results of Neat PSF Membrane, Before and After Adsorption of 1 wt% ZnO.GO MMM

Element	Composition (wt%)		
	Neat PSF membrane	**1 wt% ZnO/GO MMM before adsorption**	**1 wt% ZnO/GO MMM after adsorption**
Carbon, C	70.25	70.96	70.40
Oxygen, O	16.43	15.01	15.87
Sulphur, S	13.32	12.87	12.90
Zinc, Zn	0.00	1.16	0.56
Cadmium, Cd	0.00	0.00	0.26

4.1.3 Adsorbed Species Analysis (FTIR)

FTIR spectra of PSF membrane and 1 wt% ZnO/GO PSF MMM are shown in Figure 4.2, Appendix F and G. The absorption peaks seen in the spectrum of polysulfone (PSF) membrane at 1150.63 cm^{-1} (O-S-O stretching), 1237.14 cm^{-1} (C-O-C stretching), and 1581.06 cm^{-1} (C-C Aromatic) are the characteristics of the sulfone group (Singh et al., 2014).

The FTIR spectra of both PSF membrane and 1 wt% ZnO/GO PSF MMM exhibit absorption peaks at 3393.24 cm^{-1} and 3421.64 cm^{-1}, respectively that refer to stretching of the OH group (Johir et at., 2016). The FTIR spectrum of the 1 wt% ZnO/GO PSF MMM will exhibit absorption peak at 463.19 cm^{-1} that refer to stretching of the ZnO group (Uysal et al., 2013) but the peak is too low and become insignificant.

The intensity of the absorption peak at 3421.64 cm^{-1} for the ZnO/GO PSF MMM is higher than the intensity of the absorption peak at 3393.24 cm^{-1} for the PSF membrane. Furthermore, the absorption peak at 3421.64 cm^{-1} for the ZnO/GO PSF MMM is wider than the absorption peak at 3393.24 cm^{-1} for the PSF membrane. This indicates that the hydroxyl groups of the ZnO/GO had contributed to the increase of the absorption peak at 3421.64 cm^{-1} for the ZnO/GO PSF MMM.

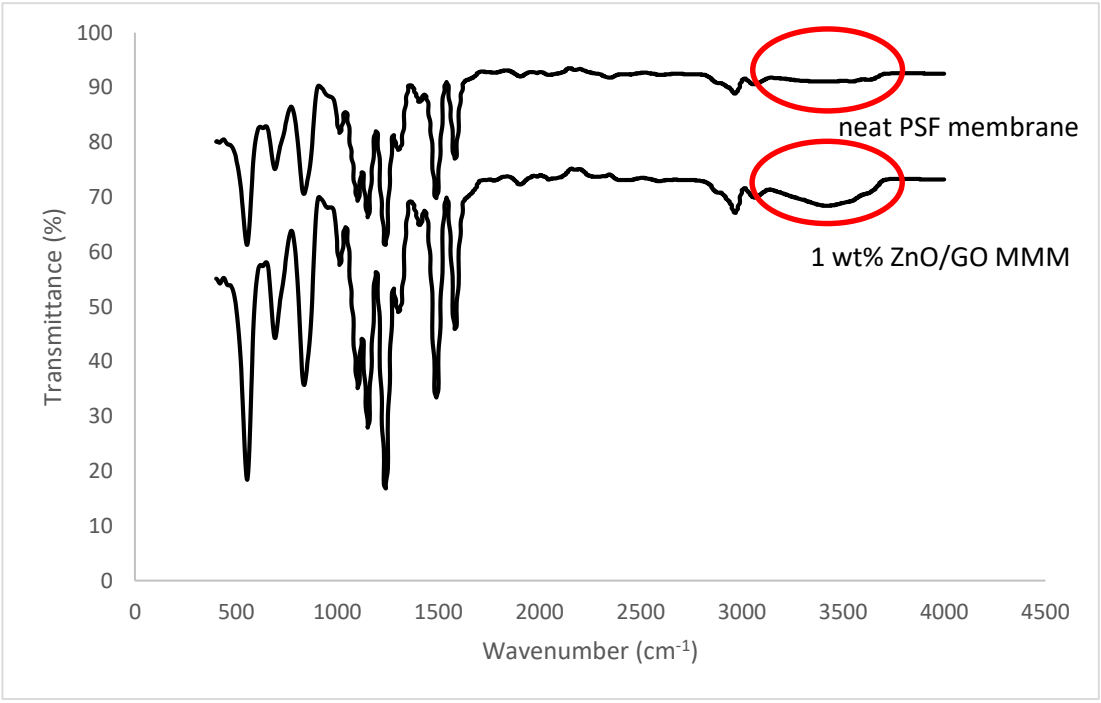

Figure 4.2: FTIR Spectra of Neat PSF membrane and 1 wt% ZnO/GO MMM

4.2 Heavy Metal Adsorption Performance Test

4.2.1 Effect of pH Conditions on Adsorption Performance

The effect of pH on the adsorption performance using 1 wt% ZnO/GO PSF MMM in the range of 2.3-11 under the initial metal concentration of 25 ppm and contact time of 3 hours is shown in Table 4.2 and Figure 4.3. A sample calculation for adsorption capacity, q_e at pH of 5.5 is shown in Appendix H. It could be observed that the adsorption capacity of Cd^{2+} increased when the pH increased from 2.3 to 5.5. The adsorption capacity is low at pH 2.3 was due to the presence of a high concentration of H^+ ions that will compete with Cd^{2+} ions (Zhang et al., 2014). The mechanism responsible for this phenomena was electronegativity which describes the tendency of an atom to attract electron towards itself. The electronegativity for H^+ and Cd^{2+} are 2.2 and 1.69, respectively, therefore H^+ had higher affinity to bind with the adsorption sites (Mark Winter, 2018).

Based on Zhang et al. (2014) findings, the adsorption capacity of Cu^{2+} on PVDF/ZnO (PZB-3) was low when the pH value was less than 4.0. This might due to the high concentration of H^+ ions that will compete with Cu^{2+} ions. A rapid increase of adsorption capacity for Cu^{2+} happened when the pH value increased from 4.0 to 6.0. However, the adsorption capacity for Cu^{2+} decreased with the increase of pH from 6.0 to 9.0 due to precipitation of Cu^{2+} ions.

At pH 5.5, the adsorption capacity is the highest. This is due to the functional group such as carboxyl (-COOH) and hydroxyl (-OH) that are responsible for binding metal ions in ZnO/GO PSF MMM will be deprotonated and hence, more divalent metal ions will bind with the negative sites (Yakout et al., 2017).

However, the adsorption capacity dropped drastically when the pH values increased over 5.5 and it reached a negative value of adsorption capacity at pH 11. This might due to the precipitation of Cd^{2+} at high pH values as shown in Figure 4.4. Since a lot of the heavy metals are amphoteric, therefore their solubility will reach a minimum at a specific pH and precipitation will occur, forming a metal hydroxide which precipitates out (Balintova and Petrilakavo, 2011). The solubility of cadmium hydroxide reached its minimum at pH 11.2 (Habib, 2017). As a result, most of the Cd^{2+} was precipitated out from the solution instead of being adsorbed on the ZnO/GO PSF MMM. Hence, the optimum pH value for the Cd^{2+} adsorption is pH 5.5.

Table 4.2: Adsorption Capacity of Cd^{2+} for Different pH Values

pH	Concentration before (ppm)	Concentration after (ppm)	Difference on the concentration (ppm)	Adsorption capacity, q_e (mg/cm^2)	q_e (x10000) (mg/cm^2)
2.3	24.67	24.63	0.04	0.0000571	0.571
3.5	26.86	26.47	0.39	0.000557	5.571
5.5	27.55	26.88	0.67	0.000957	9.571
8.3	25.6	25.26	0.34	0.000486	4.857
10	11.34	11.31	0.03	0.0000429	0.429
11	-4.878	-4.86	-0.018	-0.0000257	-0.257

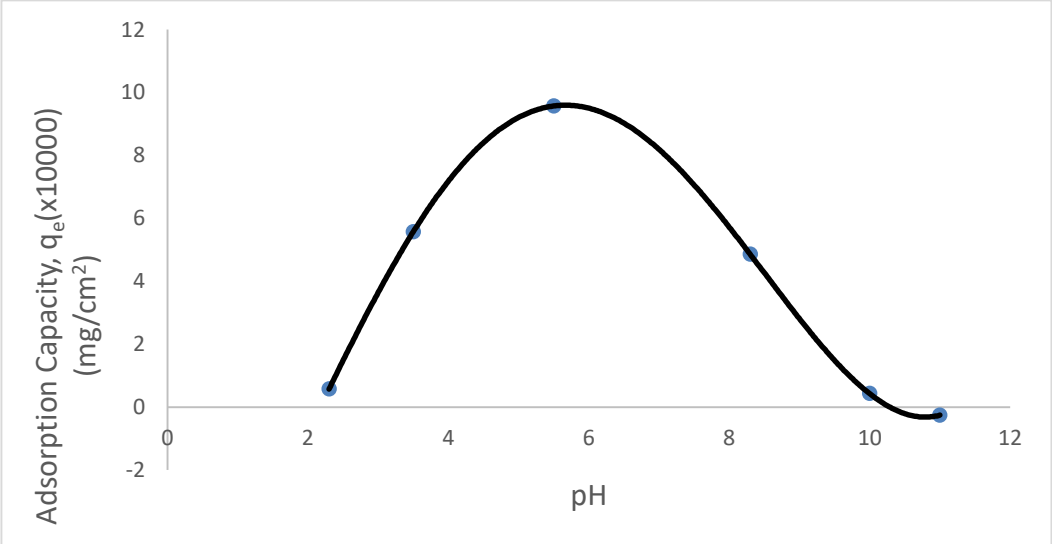

Figure 4.3: Adsorption Capacity of Cd^{2+} for Different pH Values

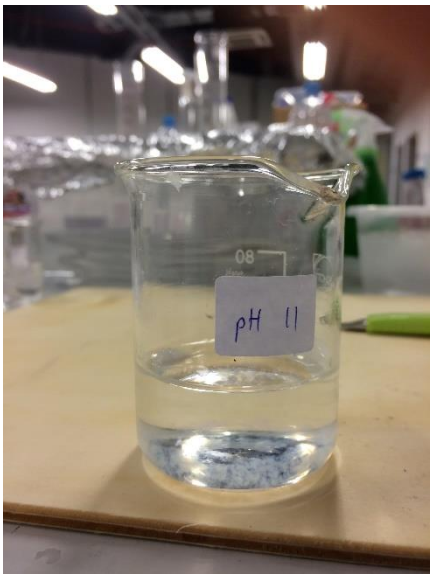

Figure 4.4: Precipitation of Cd^{2+} at pH 11

4.2.2 Effect of Contact Time on Adsorption Performance

The effect of contact time on the adsorption performance using 1 wt% ZnO/GO PSF MMM in the range of 0-4 hours under the initial metal concentration of 25 ppm and pH of 5.5 is shown in Table 4.3 and Figure 4.5. There are two interaction stages between the Cd^{2+} and adsorbent. A rapid increase in the Cd^{2+} removals onto the adsorbents in the first stage and the second stage indicates the equilibrium. The first stage is ranged from 0 to 3 hours and the second stage is ranged from 3 to 4 hours. The rapid adsorption rates in the first stage were due to the sufficient number of adsorption sites for Cd^{2+} to be adsorbed and most of the adsorption sites still remain unsaturated. In the second stage, the adsorption rate had reduced and almost reached a constant value. This indicates that the adsorption process had reached equilibrium and almost all of the adsorption sites had been fully occupied. As a result, the optimum adsorption time was 3 hours. A sample calculation for adsorption capacity at time t, q_t for 3 hours contact time is shown in Appendix I.

Based on Yakout et al. (2017) findings, a similar trend could be found by using cross-linking GO with grafted cellulose copolymer with ethylenediamine (g-C-EN) for the adsorption of Cu^{2+} and Pb^{2+}. There are two interaction stages between the metal ions and adsorbents. A rapid increase in the metal ion removals onto the adsorbents in the first stage and the second stage indicates the equilibrium.

Table 4.3: Adsorption Capacity of Cd^{2+} for Different Contact Time

Contact time	Concentration before (ppm)	Concentration after (ppm)	Difference on the concentration (ppm)	Adsorption capacity at time *t*, q_t (mg/cm^2)	q_t (x1000) (mg/cm^2)
1	28.08	27.88	0.20	0.000286	0.286
2	28.15	27.85	0.30	0.000429	0.429
3	28.10	27.72	0.38	0.000543	0.543
4	28.06	27.70	0.36	0.000514	0.514

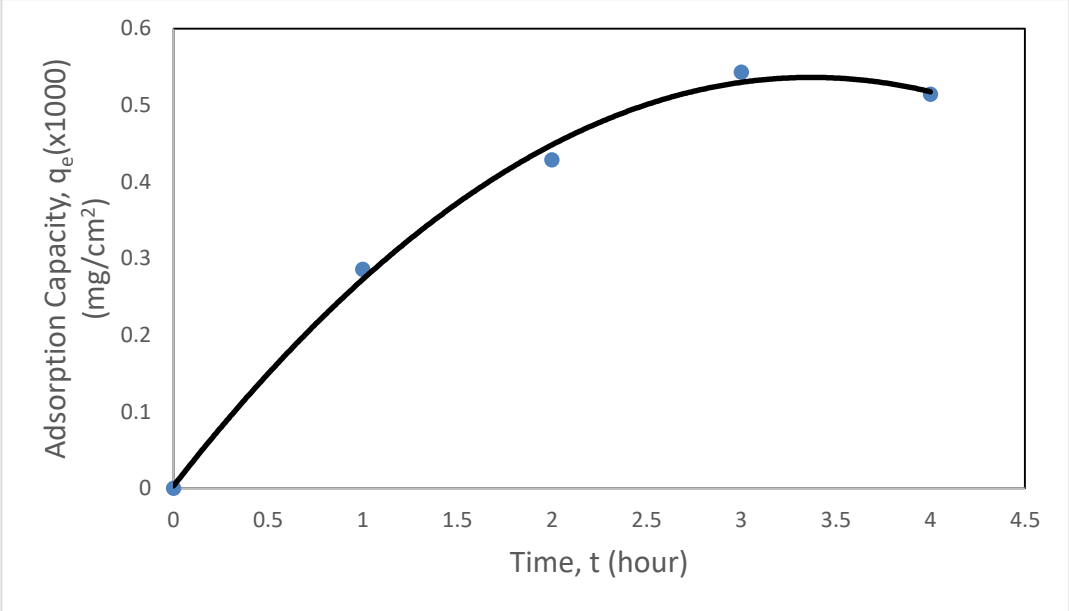

Figure 4.5: Adsorption Capacity of Cd^{2+} for Different Contact Time

4.2.3 Effect of Initial Concentration of Cd^{2+} on Adsorption Performance

The effect of initial concentration of Cd^{2+} on the adsorption performance using 1 wt% ZnO/GO PSF MMM in the range of 5-25 ppm under the pH of 5.5 and contact time of 3 hours is shown in Table 4.4 and Figure 4.6. The adsorption capacity of Cd^{2+} increased rapidly from the initial concentration of 5 ppm to 25 ppm. This is due to the enhancement in driving force by increasing the initial feed concentration of Cd^{2+} accelerated the diffusion rate of metal ions which resulted in increasing adsorption capacity of Cd^{2+} (Koushkbaghi et al., 2017). As a result, the optimum initial concentration of Cd^{2+} was 25 ppm as it achieved the highest adsorption capacity.

Koushkbaghi et al. (2017) reported that the adsorption capacity of Cr(VI) and Pb(II) by aminated-Fe_3O_4 nanoparticles filled chitosan/PVA/PES dual layers nanofibrous membrane increased when the initial concentration of Cr(VI) and Pb(II) increased from 20 to 100 ppm. By increasing the metal ions concentration, the enhancement in driving force speeded up the diffusion rate of metal ions which resulted in increasing metal ions recovery (Koushkbaghi et al., 2017).

Table 4.4: Adsorption Capacity of Cd^{2+} for Different Initial Feed Values

Initial feed (ppm)	**Concentration before (ppm)**	**Concentration after (ppm)**	**Difference on the concentration (ppm)**	**Adsorption capacity, q_e (mg/cm^2)**	**q_e (x1000) (mg/cm^2)**
5	6.01	5.74	0.27	0.000386	0.386
10	11.96	11.60	0.36	0.000514	0.514
15	17.73	17.35	0.38	0.000543	0.543
20	21.85	21.44	0.41	0.000586	0.586
25	28.77	28.35	0.42	0.000600	0.600

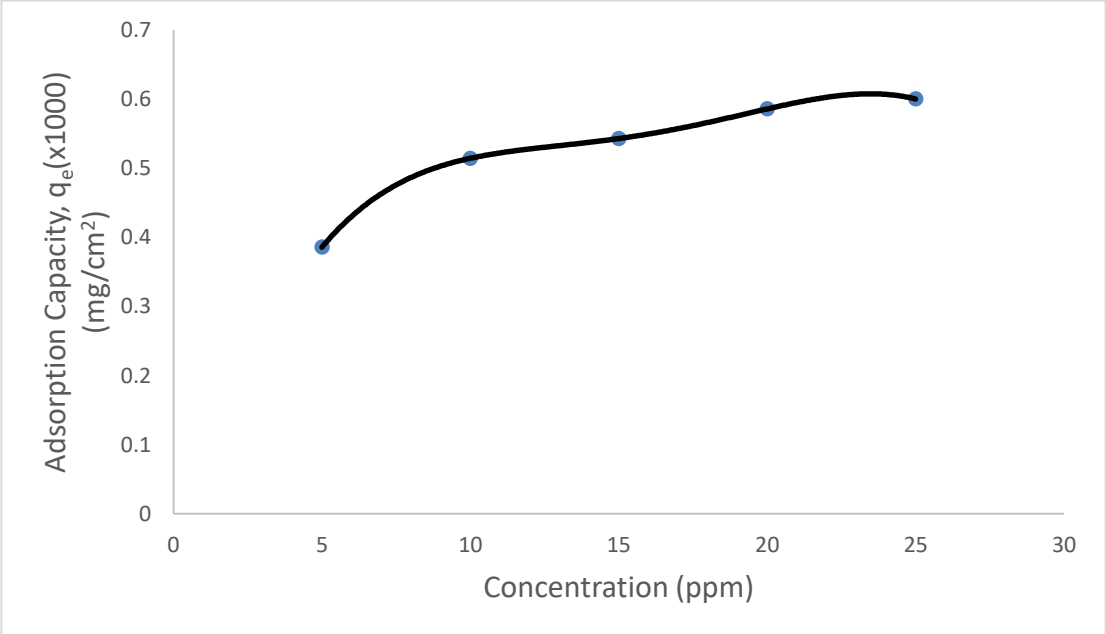

Figure 4.6: Adsorption Capacity of Cd^{2+} for Different Initial Feed Values

4.2.4 Effect of Number of Membranes on Adsorption Performance

The effect of the number of membranes on the adsorption performance using 1 wt% ZnO/GO PSF MMM in the range of 1-5 under the initial metal concentration of 25 ppm, pH 5.5 and contact time of 3 hours is shown in Table 4.5 and Figure 4.7. A sample calculation for difference per membrane (ppm) and adsorption per area membrane (ppm/cm^2) is shown in Appendix J and the results generated from the ICP-OES for different number of membranes is shown in Appendix K. The concentrations after the adsorption reduced greatly as the number of membranes increased. This is because more adsorption sites were available for the adsorption as the number of membranes increased. The average concentration adsorbed by each membrane was 0.49 ppm and the adsorption per area membrane was 0.07 ppm/cm^2. This result will be used and further discussed in section 4.6 (Bulk Analysis).

Table 4.5: Adsorption Capacity of Cd^{2+} for Different Number of Membrane

Number of membrane	**Concentration before (ppm)**	**Concentration after (ppm)**	**Difference (ppm)**	**Difference per membrane (ppm)**	**Adsorption per area membrane (ppm/cm^2)**
1	26.32	25.89	0.43	0.430	0.0614
2	26.32	25.26	1.06	0.530	0.0757
3	26.32	24.83	1.49	0.497	0.0710
4	26.32	24.48	1.84	0.460	0.0657
5	26.32	23.65	2.67	0.534	0.0763
			Average	0.490	0.0700

Note: The membrane area is 7 cm^2 (1 cm x 7 cm).

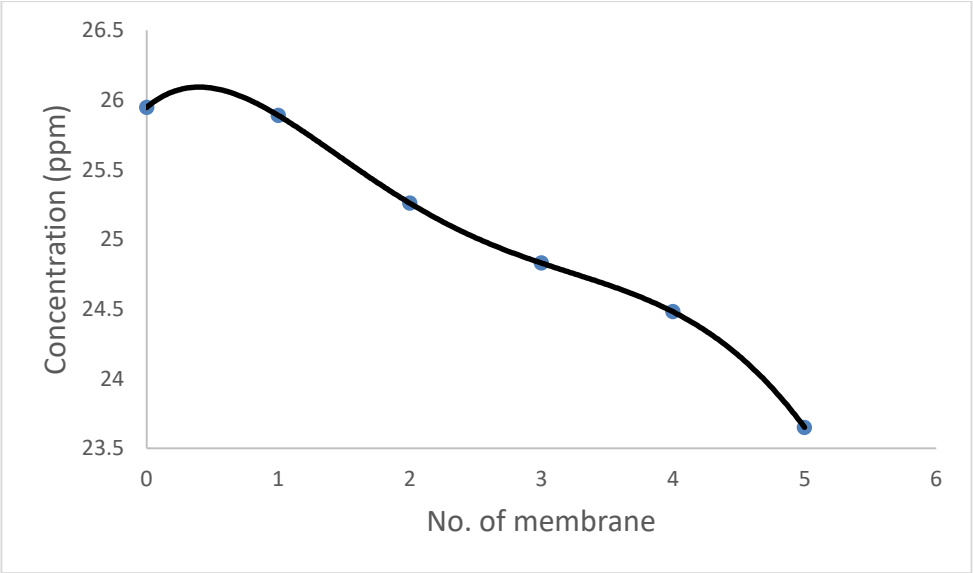

Figure 4.7: Adsorption Capacity of Cd^{2+} for Different Number of Membrane

4.2.5 Effect of Humic Acid on Adsorption Performance

The effect of humic acid on the adsorption performance using 1 wt% ZnO/GO PSF MMM under the initial metal concentration of 20 ppm and contact time of 3 hours is shown in Table 4.6. The initial metal concentration was 20 ppm due to the dilution effect of humic acid. The amount of adsorbed Cd^{2+} on the membrane was greatly reduced by 47.37% when humic acid existed because humic acid structure encompasses mainly, both aromatic and aliphatic organic compounds which constitute three main functional groups such as carboxylic acids, methoxy carbonyls and phenolic alcohols that will compete with ZnO/GO PSF MMM for the adsorption of Cd^{2+} (Thuyavan et al., 2014).

Sounthararajah et al. (2015) reported that adding humic acid into the heavy metal solution reduced the efficiency in removing Cd^{2+} by granular activated carbon. The efficiency was reduced by 20% due to humic acid compete with granular activated carbon for the adsorption of Cd^{2+}.

Table 4.6: Amount of Adsorbed Cd^2 With and Without Humic Acid

	20 ppm of Cd^2 (without humic acid)	**20 ppm of Cd^2 (with humic acid)**
Before adsorption	21.85 ppm	20.53 ppm
After adsorption	21.47 ppm	20.33 ppm
Amount of adsorbed Cd^2	0.38 ppm	0.20 ppm
Adsorption per area membrane (ppm/cm^2)	0.0543	0.0286

Note: The membrane area is 7 cm^2 (1 cm x 7 cm).

4.3 Langmuir and Freundlich Adsorption Isotherm

Figure 4.8 and Figure 4.9 show the plot of Langmuir adsorption isotherm. The adsorption behaviour of Cd^{2+} best described by using Langmuir model as shown in the equation 3.4 because the coefficient of determination, R^2 which was 0.9983 is higher than the coefficient of determination which was 0.9511 in Freundlich adsorption isotherm. This model assumed that the rate of adsorption and desorption in any layer are the same and molecules adsorb on equivalent adsorption sites in the first layer (Khan et al., 2013). It also describes the interactions between adsorbate-adsorbate are ignored (Khan et al., 2013). Based on the equation 3.4, $1/q_{max}$ was the gradient of the slope and the value was 1433.3 where q_{max} was the maximum adsorption capacity for adsorption of Cd^{2+} in mg/cm^2. The reciprocal of the slope gradient would provide the maximum adsorption capacity for adsorption of Cd^{2+}. Once the maximum adsorption capacity for adsorption of Cd^{2+} was determined, the Langmuir constants of adsorption, b then could be calculated. Hence, the q_{max} was 0.000698 mg/cm^2 and the Langmuir constants of adsorption was 0.2227 L/mg.

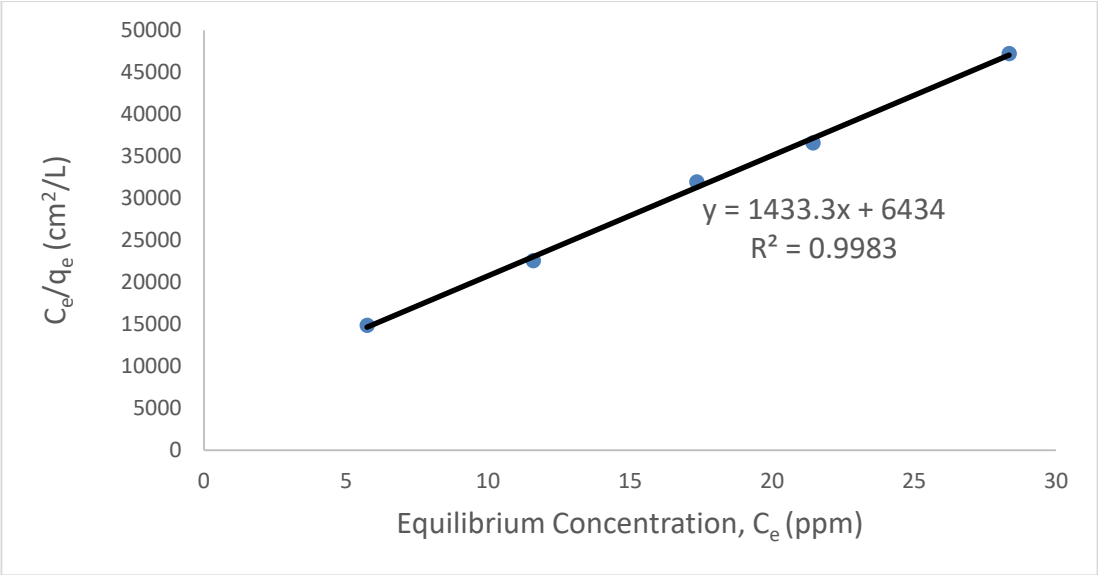

Figure 4.8: Langmuir Adsorption Isotherm

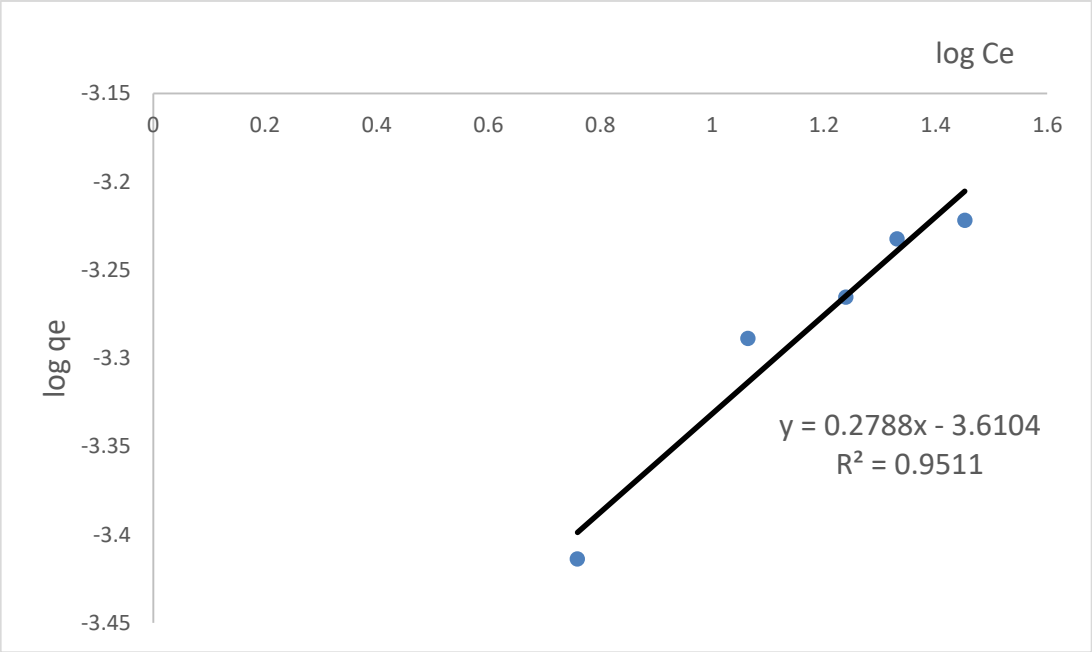

Figure 4.9: Freundlich Adsorption Isotherm

4.4 Adsorption Kinetics

Pseudo-first and second order kinetic models were used to describe the kinetic adsorption process. The plots of pseudo-first and second order kinetic models are shown in Figure 4.10 and 4.11. Based on the figures, pseudo-second order exhibited a higher coefficient of determination, R^2 which was 0.9553. Hence, pseudo-second order kinetic model is the most applicable model to describe the adsorption process of cadmium ions by the ZnO/GO MMM. Pseudo-second order kinetic model assumes that chemisorption is the rate determining step and the adsorbates (Cd^{2+}) and adsorbents (ZnO/GO) were chemically bonded together (Old.iupac.org, 2018).

From equation 3.6, the slope gradient of pseudo-second order kinetic model was $1/q_{eq}$ and the value was 1369.3 where q_{eq} was the equilibrium adsorption capacity for adsorption of Cd^{2+} in mg/cm^2. The reciprocal of the slope gradient would provide the equilibrium adsorption capacity for adsorption of Cd^{2+}. Once the equilibrium adsorption capacity for adsorption of Cd^{2+} was determined, the rate constant for pseudo-second order, k_2 in cm^2/mg.h then could be calculated. Hence, the q_{eq} was 0.00073 mg/cm^2 and the rate constant for pseudo-second order was 964.3 cm^2/mg.h at 25 ppm of Cd^{2+} solution.

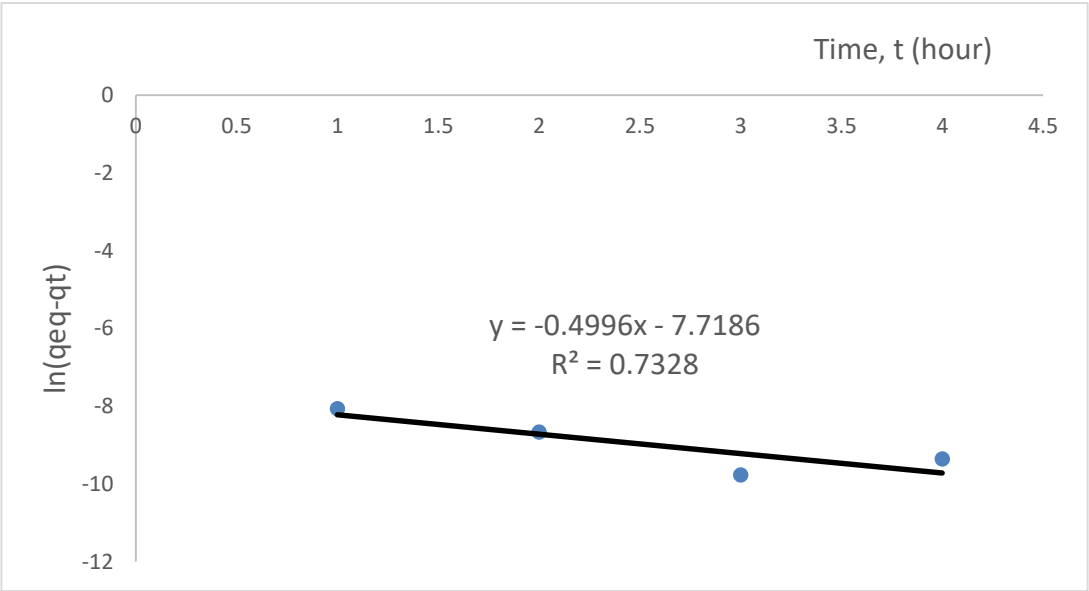

Figure 4.10: Pseudo First Order Kinetic Model

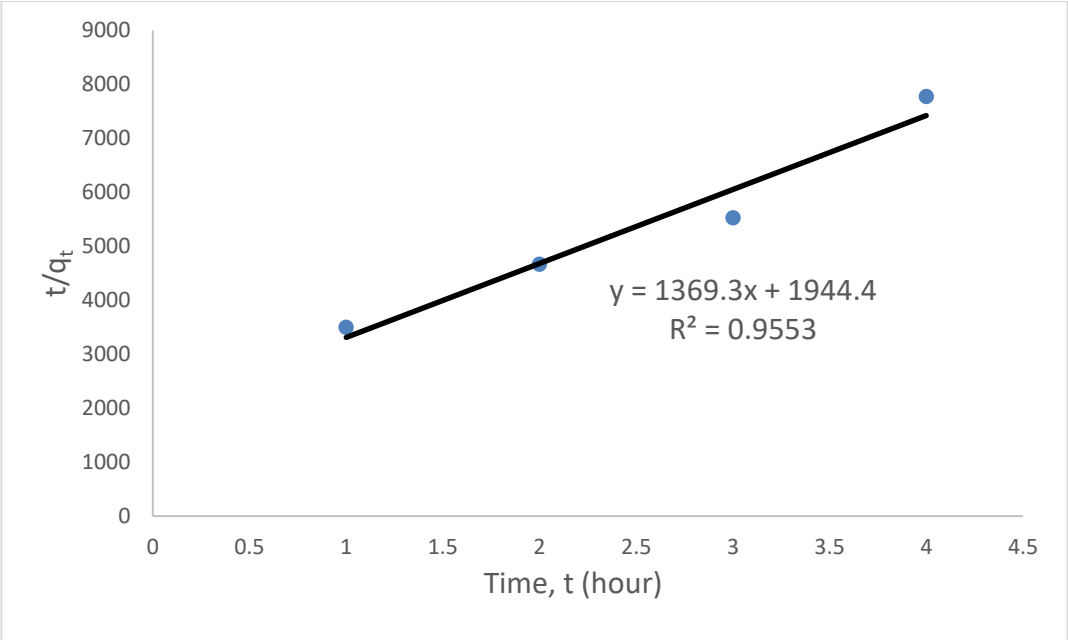

Figure 4.11: Pseudo Second Order Kinetic Model

4.5 Desorption and Regeneration

0.1 M HCl was used to regenerate the membrane that undergone the adsorption process under the optimum operating conditions of pH 5.5, the initial concentration of 25 ppm and contact time of 3 hours. Three cycles of desorption and regeneration were applied to investigate the desorption performance of the membrane and the result is shown in Table 4.7. A sample calculation for the percentage of regeneration at cycle 3 is shown in Appendix L. Based on Table 4.7, the membrane shows good desorption performance because it maintained the adsorption efficiency. The percentage of regeneration still remain above 90% after 3 cycles of desorption and regeneration. Furthermore, the results in Table 4.8 proven that the membrane was successfully regenerated as the Cd^{2+} ions were present in the HCl solution. The first cycle of desorption and regeneration was based on adsorbed Cd^{2+} in Table 4.4 which is 0.42 ppm at 25 ppm of initial feed concentration.

Table 4.7: Desorption Performance of the Membrane

Cycle	Concentration before (ppm)	Concentration after (ppm)	Difference (ppm)	Percentage of regeneration
1	26.78	26.36	0.42	100%
2	26.78	26.37	0.41	97.62%
3	26.78	26.40	0.38	90.48%

Table 4.8: Amount of Cd^{2+} in HCl for Each Cycle

Cycle	Amount of Cd^{2+} in HCl (ppm)
1	0.308
2	0.247
3	0.283

4.6 Bulk Analysis

A bulk analysis was conducted to study the adsorption performance of the ZnO/GO in both MMMs and bulk. The result obtained is being compared with the result in section 4.2.4 (Effect of Number of Membranes on Adsorption Performance) and it is shown in Table 4.9. The obtained amount of adsorbed Cd^{2+} in bulk was based on the initial Cd^{2+} concentration of 92.53 ppm, the final Cd^{2+} concentration of 42.63 ppm and 0.13 g of ZnO/GO that had been used. The obtained amount of adsorbed Cd^{2+} in the membrane was based on 0.49 ppm average adsorbed Cd^{2+} (from section 4.2.4), 780 cm^2 (3 x 20 cm x 13 cm) of total membrane area and 0.1 g of ZnO/GO that had been used to cast the membranes. A sample calculation for amount of adsorbed Cd^{2+} per weight of ZnO/GO is shown in Appendix M. The adsorbed Cd^{2+} in membrane per weight of ZnO/GO is higher than the adsorbed Cd^{2+} in bulk per weight of ZnO/GO because nano-adsorbents in the suspension will cause the agglomeration in aqueous solution during the adsorption process (Koushkbaghi et al., 2017). Hence, less active sites will be available for the process of adsorption.

Table 4.9: Amount of Adsorbed Cd^{2+} Per Weight of ZnO/GO

Adsorbed Cd^{2+} in membrane per weight of ZnO/GO (ppm/g)	**Adsorbed Cd^{2+} in bulk per weight of ZnO/GO (ppm/g)**
546.02	383.85

CHAPTER 5

CONCLUSIONS AND RECOMMENDATIONS

5.1 Conclusions

The objectives of this research were to fabricate and characterize the neat PSF membranes and 1 wt% ZnO/GO PSF MMMs. The adsorption performances of cadmium ions, Cd^{2+} by 1 wt% ZnO/GO PSF MMMs under different pH conditions, contact time, number of membranes and initial concentration of Cd^{2+} were studied. Besides that, the effect of the addition of an organic matter, humic acid on the adsorption performances of cadmium ions, Cd^{2+} by 1 wt% ZnO/GO PSF MMMs under the optimum condition was also studied and the adsorption model for Cd^{2+} adsorption using 1 wt% ZnO/GO PSF MMMs was determined. Moreover, this research also studied the desorption and regeneration performance of the 1 wt% ZnO/GO PSF MMM using 0.1 M of hydrochloric acid under the optimum condition. In addition, a bulk analysis was conducted to study the adsorption performance of the ZnO/GO in both MMMs and bulk.

Neat PSF membranes and 1 wt% ZnO/GO PSF MMMs were fabricated by using the phase inversion method in this research. The surface morphology of the neat PSF and 1 wt% ZnO/GO PSF MMM were observed using SEM and a short asymmetric finger like pore structures were formed at the upper layer and followed by porous sub-layer contained macro-voids at the bottom layer. The pore size for the 1 wt% ZnO/GO PSF MMM is larger than the neat PSF membrane because the oxygen functional groups of the ZnO/GO had attracted the non-solvent towards the polymer solution resulting in an enhanced inflow of non-solvent and outflow of solvent. Therefore, the phase inversion process was accelerated (Chong et al., 2017). Elemental analysis, energy dispersive X-ray spectroscopy (EDX) had proven that the presence of ZnO nanoparticles in the 1 wt% ZnO/GO PSF MMMs and also showed that Cd^{2+} had been adsorbed on the surface of the MMM. Besides, FTIR spectra of PSF membrane and 1 wt% ZnO/GO PSF MMM had proven that the presence of ZnO and GO in the ZnO/GO PSF MMM due to more intense and wider absorption peaks that refer to stretching of the OH group.

The optimum pH value for the Cd^{2+} adsorption was pH 5.5 and the optimum contact time was 3 hours as it had reached equilibrium. In addition, the optimum initial

concentration of Cd^{2+} was 25 ppm as it achieved the highest adsorption capacity and the increase of the number of membranes will lead to higher adsorption capacity as more adsorption sites were available for the adsorption. The amount of adsorbed Cd^{2+} was greatly reduced when humic acid existed due to humic acid will compete with ZnO/GO PSF MMM for the adsorption of Cd^{2+}.

It was best described by using the Langmuir model because the coefficient of determination, R^2 which was 0.9983 is higher than the coefficient of determination which was 0.9511 in Freundlich adsorption isotherm. According to Langmuir adsorption isotherm, the q_{max} obtained was 0.000698 mg/cm^2 and the Langmuir constant of adsorption was 0.2227 L/mg. Furthermore, pseudo-second order exhibited a higher coefficient of determination, R^2 which was 0.9553 and it was assumed that chemisorption is the rate determining step and the adsorbates (Cd^{2+}) and adsorbents (ZnO/GO) were chemically bonded together (Old.iupac.org, 2018). According to pseudo-second order kinetic model, the q_{eq} obtained was 0.00073 mg/cm^2 and the rate constant for pseudo-second order was 964.3 cm^2/mg.h at 25 ppm of Cd^{2+} solution.

Three cycles of desorption and regeneration were applied to investigate the desorption performance of the membrane and the result showed that the membrane shows good desorption performance because it had maintained the adsorption efficiency. Last but not the least, the bulk analysis showed that the adsorbed Cd^{2+} in membrane per weight of ZnO/GO is higher than the adsorbed Cd^{2+} in bulk per weight of ZnO/GO because nano-adsorbents in the suspension will cause the agglomeration in aqueous solution during the adsorption process. In a nutshell, ZnO/GO PSF MMMs have high applicability in the removal of heavy metal ions due to its simplicity and flexibility of design, high removal of heavy metal ions, good desorption and regeneration performance and ease of operation.

5.2 Recommendations

There are some recommendations that can be further studied in the future in order to understand well the application of nanoparticles MMMs in heavy metal removal.

(i) To study the adsorption performance using different types of heavy metal ions such as Pb^{2+}, Cu^{2+}, Ni^{2+} and etc.

(ii) To study the adsorption performance of heavy metal ions using different combinations of hybrid nanoparticles.

(iii) Use a higher dosage of adsorbent in order to achieve better adsorption capacity.

(iv) Perform the adsorption test using the wastewater from the industry such as car manufacturing and electroplating.

REFERENCES

Al-Rashdi, B., Somerfield, C. and Hilal, N. (2011). Heavy Metals Removal Using Adsorption and Nanofiltration Techniques. *Separation & Purification Reviews*, 40(3), pp.209-259.

Al-Malack, M. and Basaleh, A. (2016). Adsorption of heavy metals using activated carbon produced from municipal organic solid waste. *Desalination and Water Treatment*, 57(51), pp.24519-24531.

Ariffin, N., Abdullah, M., Mohd Arif Zainol, M., Murshed, M., Hariz-Zain, Faris, M. and Bayuaji, R. (2017). Review on Adsorption of Heavy Metal in Wastewater by Using Geopolymer. *MATEC Web of Conferences*, 97, p.01023.

Aimi, b., Norhafizah, b. and Wong, C. (2013). Removal of Cu(II) from Water by Adsorption on Chicken Eggshell. *International Journal of Engineering & Technology IJET-IJENS*, 13(1).

Ainscough, T., Alagappan, P., Oatley-Radcliffe, D. and Barron, A. (2017). A hybrid super hydrophilic ceramic membrane and carbon nanotube adsorption process for clean water production and heavy metal removal and recovery in remote locations. *Journal of Water Process Engineering*, 19, pp.220-230.

Al-Malack, M. and Basaleh, A. (2016). Adsorption of heavy metals using activated carbon produced from municipal organic solid waste. *Desalination and Water Treatment*, 57(51), pp.24519-24531.

Barkhordar, B. and Ghiasseddin, M. (2004). Comparision of Langmuir and Freundlich Equilibriums in Cr, Cu and Ni Adsorption by Sargassum. *Iranian J Env Health Sci En*, 1(2), pp.58-64.

Barakat, M. (2011). New trends in removing heavy metals from industrial wastewater. *Arabian Journal of Chemistry*, 4(4), pp.361-377.

Balintova, M. and Petrilakova, A. (2011). Study of pH Influence on Selective Precipitation of Heavy Metals from Acid Mine Drainage. *Chemical Engineering Transactions*, 25, pp.345-350.

Chong, W., Mahmoudi, E., Chung, Y., Koo, C., Mohammad, A. and Kamarudin, K. (2017). Improving performance in algal organic matter filtration using polyvinylidene fluoride–graphene oxide nanohybrid membranes. *Algal Research*, 27, pp.32-42.

Chong, W., Mahmoudi, E., Chung, Y., Ba-Abbad, M., Koo, C. and Mohammad, A. (2017). Polyvinylidene fluoride membranes with enhanced antibacterial and low fouling properties by incorporating ZnO/rGO composites. *DESALINATION AND WATER TREATMENT*, 96, pp.12-21.

Chung, Y., Mahmoudi, E., Mohammad, A., Benamor, A., Johnson, D. and Hilal, N. (2017). Development of polysulfone-nanohybrid membranes using ZnO-GO composite for enhanced antifouling and antibacterial control. *Desalination*, 402, pp.123-132.

Fang, X., Li, J., Li, X., Pan, S., Zhang, X., Sun, X., Shen, J., Han, W. and Wang, L. (2017). Internal pore decoration with polydopamine nanoparticle on polymeric ultrafiltration membrane for enhanced heavy metal removal. *Chemical Engineering Journal*, 314, pp.38-49.

Fu, F. and Wang, Q. (2011). Removal of heavy metal ions from wastewaters: A review. *Journal of Environmental Management*, 92(3), pp.407-418.

Gunatilake, S. (2015). Methods of Removing Heavy Metals from Industrial Wastewater. *Journal of Multidisciplinary Engineering Science Studies (JMESS)*, 1(1), pp.12-15.

Goldberg, S. (2013). *Surface Complexation Modeling*. Reference Module in Earth Systems and Environmental Sciences.

Habib, K. (2017). Effect of pH and Initial pb(II) Concentration on The Lead Removal Efficiency from Industrial Wastewater Using Ca(OH)2. *International Journal of Water and Wastewater Treatment*, 3(2).

Huang, H. and Yang, S. (2006). Filtration characteristics of polysulfone membrane filters. *Journal of Aerosol Science*, 37(10), pp.1198-1208.

He, J., Cai, X., Chen, K., Li, Y., Zhang, K., Jin, Z., Meng, F., Liu, N., Wang, X., Kong, L., Huang, X. and Liu, J. (2016). Performance of a novelly-defined zirconium metal-organic frameworks adsorption membrane in fluoride removal. *Journal of Colloid and Interface Science*, 484, pp.162-172.

Johir, M., Pradhan, M., Loganathan, P., Kandasamy, J. and Vigneswaran, S. (2016). Phosphate adsorption from wastewater using zirconium (IV) hydroxide: Kinetics, thermodynamics and membrane filtration adsorption hybrid system studies. *Journal of Environmental Management*, 167, pp.167-174.

Khan, S., Rahman, M., Marwani, H., Asiri, A. and Alamry, K. (2013). An assessment of zinc oxide nanosheets as a selective adsorbent for cadmium. *Nanoscale Research Letters*, 8(1), p.377.

Koushkbaghi, S., Zakialamdari, A., Pishnamazi, M., Ramandi, H., Aliabadi, M. and Irani, M. (2017). Aminated-Fe 3 O 4 nanoparticles filled chitosan/PVA/PES dual layers nanofibrous membrane for the removal of Cr(VI) and Pb(II) ions from aqueous solutions in adsorption and membrane processes. *Chemical Engineering Journal*.

Kolbasov, A., Sinha-Ray, S., Yarin, A. and Pourdeyhimi, B. (2017). Heavy metal adsorption on solution-blown biopolymer nanofiber membranes. *Journal of Membrane Science*, 530, pp.250-263.

Li Li (2018). *3.2 Surface Complexation Models (SCMs) | PNG 550: Reactive Transport in the Subsurface*. [online] E-education.psu.edu. Available at: https://www.e-education.psu.edu/png550/node/583 [Accessed 14 Aug. 2018].

Mark Winter, U. (2018). *WebElements Periodic Table » Cadmium » electronegativity*. [online] Webelements.com. Available at: https://www.webelements.com/cadmium/electronegativity.html [Accessed 16 Aug. 2018].

Majewska-Nowak, K. (1989). Synthesis and properties of polysulfone membranes. *Desalination*, 71(2), pp.83-95.

Mashangwa, T., Tekere, M. and Sibanda, T. (2017). Determination of the Efficacy of Eggshell as a Low-Cost Adsorbent for the Treatment of Metal Laden Effluents. *International Journal of Environmental Research*, 11(2), pp.175-188.

Maximous, N., Nakhla, G. and Wan, W. (2010). Removal of Heavy Metals from Wastewater by Adsorption and Membrane Processes: a Comparative Study. *International Scholarly and Scientific Research & Innovation*, 4(4).

Mee-inc.com. (2018). *Energy Dispersive X-Ray Spectroscopy | EDS Failure Analysis | EDS Material Analysis | EDX Failure Analysis | EDX Material Analysis*. [online] Available at: https://www.mee-inc.com/hamm/energy-dispersive-x-ray-spectroscopyeds/ [Accessed 7 Apr. 2018].

Mondal, M., Dutta, M. and De, S. (2017). A novel ultrafiltration grade nickel iron oxide doped hollow fiber mixed matrix membrane: Spinning, characterization and application in heavy metal removal. *Separation and Purification Technology*, 188, pp.155-166.

Mukherjee, R., Bhunia, P. and De, S. (2016). Impact of graphene oxide on removal of heavy metals using mixed matrix membrane. *Chemical Engineering Journal*, 292, pp.284-297.

Old.iupac.org. (2018). *Chemisorption and physisorption*. [online] Available at: http://old.iupac.org/reports/2001/colloid_2001/manual_of_s_and_t/node16.html [Accessed 10 Apr. 2018].

Park, H., Kwak, S., Mahardika, D., Mameda, N. and Choo, K. (2017). Mixed metal oxide coated polymer beads for enhanced phosphorus removal from membrane bioreactor effluents. *Chemical Engineering Journal*, 319, pp.240-247.

Peng, W., Li, H., Liu, Y. and Song, S. (2017). A review on heavy metal ions adsorption from water by graphene oxide and its composites. *Journal of Molecular Liquids*, 230, pp.496-504.

Phelane, L. (2013). Metal Nanoparticle Modified Polysulfone Membrane For Water Treatment.

Pimentel, G. (1960). Infrared spectroscopy: A chemist's tool. *Journal of Chemical Education*, 37(12), p.651.

Pourbeyram, S. (2016). Effective Removal of Heavy Metals from Aqueous Solutions by Graphene Oxide–Zirconium Phosphate (GO–Zr-P) Nanocomposite. *Industrial & Engineering Chemistry Research*, 55(19), pp.5608-5617.

Polymerdatabase.com. (2018). *Properties of Polysulfones*. [online] Available at: http://polymerdatabase.com/polymer%20classes/Polysulfone%20type.html [Accessed 3 Apr. 2018].

Richards, H., Baker, P. and Iwuoha, E. (2012). Metal Nanoparticle Modified Polysulfone Membranes for Use in Wastewater Treatment: A Critical Review. *Journal of Surface Engineered Materials and Advanced Technology*, 02(03), pp.183-193.

Rtilab.com. (2018). *FTIR Analysis | RTI Laboratories*. [online] Available at: http://rtilab.com/techniques/ftir-analysis/ [Accessed 13 Aug. 2018].

Shariful, M., Sharif, S., Lee, J., Habiba, U., Ang, B. and Amalina, M. (2017). Adsorption of divalent heavy metal ion by mesoporous-high surface area chitosan/poly (ethylene oxide) nanofibrous membrane. *Carbohydrate Polymers*, 157, pp.57-64.

Singh, K., Devi, S., Bajaj, H., Ingole, P., Choudhari, J. and Bhrambhatt, H. (2014). Optical Resolution of Racemic Mixtures of Amino Acids through Nanofiltration Membrane Process. *Separation Science and Technology*, 49(17), pp.2630-2641.

Sounthararajah, D., Loganathan, P., Kandasamy, J. and Vigneswaran, S. (2015). Effects of Humic Acid and Suspended Solids on the Removal of Heavy Metals from Water by Adsorption onto Granular Activated Carbon. *International Journal of Environmental Research and Public Health*, 12(9), pp.10475-10489.

Tiron, L., Pintilie, Ș., Vlad, M., Birsan, I. and Baltă, Ș. (2017). Characterization of Polysulfone Membranes Prepared with Thermally Induced Phase Separation Technique. *IOP Conference Series: Materials Science and Engineering*, 209, p.012013.

Thuyavan, Y., Anantharaman, N., Arthanareeswaran, G. and Ismail, A. (2014). Adsorptive Removal of Humic Acid by Zirconia Embedded in a Poly(ether sulfone) Membrane. *Industrial & Engineering Chemistry Research*, 53(28), pp.11355-11364.

Upadhyay, R., Soin, N. and Roy, S. (2014). Role of graphene/metal oxide composites as photocatalysts, adsorbents and disinfectants in water treatment: a review. *RSC Adv.*, 4(8), pp.3823-3851.

Uysal, I., Severcan, F. and Evis, Z. (2013). Characterization by Fourier transform infrared spectroscopy of hydroxyapatite co-doped with zinc and fluoride. *Ceramics International*, 39(7), pp.7727-7733.

Vinodhini, P. and Sudha, P. (2016). Removal of heavy metal chromium from tannery effluent using ultrafiltration membrane. *Textiles and Clothing Sustainability*, 2(1).

Wang, J., Huang, T., Zhang, L., Yu, Q. and Hou, L. (2018). *Dopamine crosslinked graphene oxide membrane for simultaneous removal of organic pollutants and trace heavy metals from aqueous solution*.

Yakout, A., El-Sokkary, R., Shreadah, M. and Abdel Hamid, O. (2017). Cross-linked graphene oxide sheets via modified extracted cellulose with high metal adsorption. *Carbohydrate Polymers*, 172, pp.20-27.

Zhang, N., Qiu, H., Si, Y., Wang, W. and Gao, J. (2011). Fabrication of highly porous biodegradable monoliths strengthened by graphene oxide and their adsorption of metal ions. *Carbon*, 49(3), pp.827-837.

Zhang, J., Chen, N., Li, M. and Feng, C. (2017). Synthesis and environmental application of zirconium–chitosan/graphene oxide membrane. *Journal of the Taiwan Institute of Chemical Engineers*, 77, pp.106-112.

Zhang, P., Gong, J., Zeng, G., Deng, C., Yang, H., Liu, H. and Huan, S. (2017). Cross-linking to prepare composite graphene oxide-framework membranes with high-flux

for dyes and heavy metal ions removal. *Chemical Engineering Journal*, 322, pp.657-666.

Zhang, X., Wang, Y., Liu, Y., Xu, J., Han, Y. and Xu, X. (2014). Preparation, performances of PVDF/ZnO hybrid membranes and their applications in the removal of copper ions. *Applied Surface Science*, 316, pp.333-340.

Zhang, L., Zhou, J., Zhou, D. and Tang, Y. (1999). Adsorption of cadmium and strontium on cellulose/alginic acid ion-exchange membrane. *Journal of Membrane Science*, 162(1-2), pp.103-109.

Zito Ray, P. and J. Shipley, H. (2015). Inorganic Nano-Adsorbents for the Removal of Heavy Metals and Arsenic: A Review. *RSC Advances*, pp.29-34.

APPENDICES

APPENDIX A: Calculation for Stock Solution Preparation

Sample calculation for stock solution preparation

$$mass\ of\ CdCl_2\ =\ V\ \text{x}\ \frac{MW\ of\ \text{Cd}Cl_2\ \text{x ppm of}\ Cd^{2+}}{MW\ of\ Cd^{2+}}\ \text{x}\ stoichiometry$$

where,

MW of $CdCl_2$= 183.329 g/mol

MW of Cd^{2+} = 112.411 g/mol

V = 1 L

ppm of Cd^{2+} = 100 ppm or 100 mg/L

$$mass\ of\ \text{Cd}Cl_2\ =\ 1\ \text{L x}\ \frac{183.329\frac{\text{g}}{\text{mol}}\text{x}\ 100\frac{\text{mg}}{\text{L}}}{112.411\frac{\text{g}}{\text{mol}}}\ \text{x}\ \frac{1\ \text{mol of Cd}^{2+}}{1\ \text{mol of Cl}_2}$$

= 163.09 mg

So, 163.09 mg of $CdCl_2$ is needed to be dissolved into 1 L of deionised water to produce 100 ppm of Cd^{2+} stock solution.

APPENDIX B: Sample Calculation for 40 ppm of Cd^{2+} Solution

Sample calculation for 40 ppm of Cd^{2+} solution

$$C_1V_1 = C_2V_2$$

By considering the desired volume of Cd^{2+} stock solution, V_2 to be the value of 60 mL and desired concentration of Cd^{2+} stock solution, C_2 to be the value of 20 ppm.

where,

C_1 = 100 ppm

C_2 = 20 ppm

V_1 = volume of Cd^{2+} stock solution required for dilution, mL

V_2 = 60 mL

$$V_1 = \frac{C_2V_2}{C_1}$$

$$= \frac{20 \text{ ppm x } 60 \text{ mL}}{100 \text{ ppm}}$$

= 12 mL

So, 12 mL of 100 ppm Cd^{2+} stock solution is needed to mix with 48 mL of deionized water in order to produce 60 mL of 20 ppm Cd^{2+} solution.

APPENDIX C: Calibration Curve for Cd^{2+}

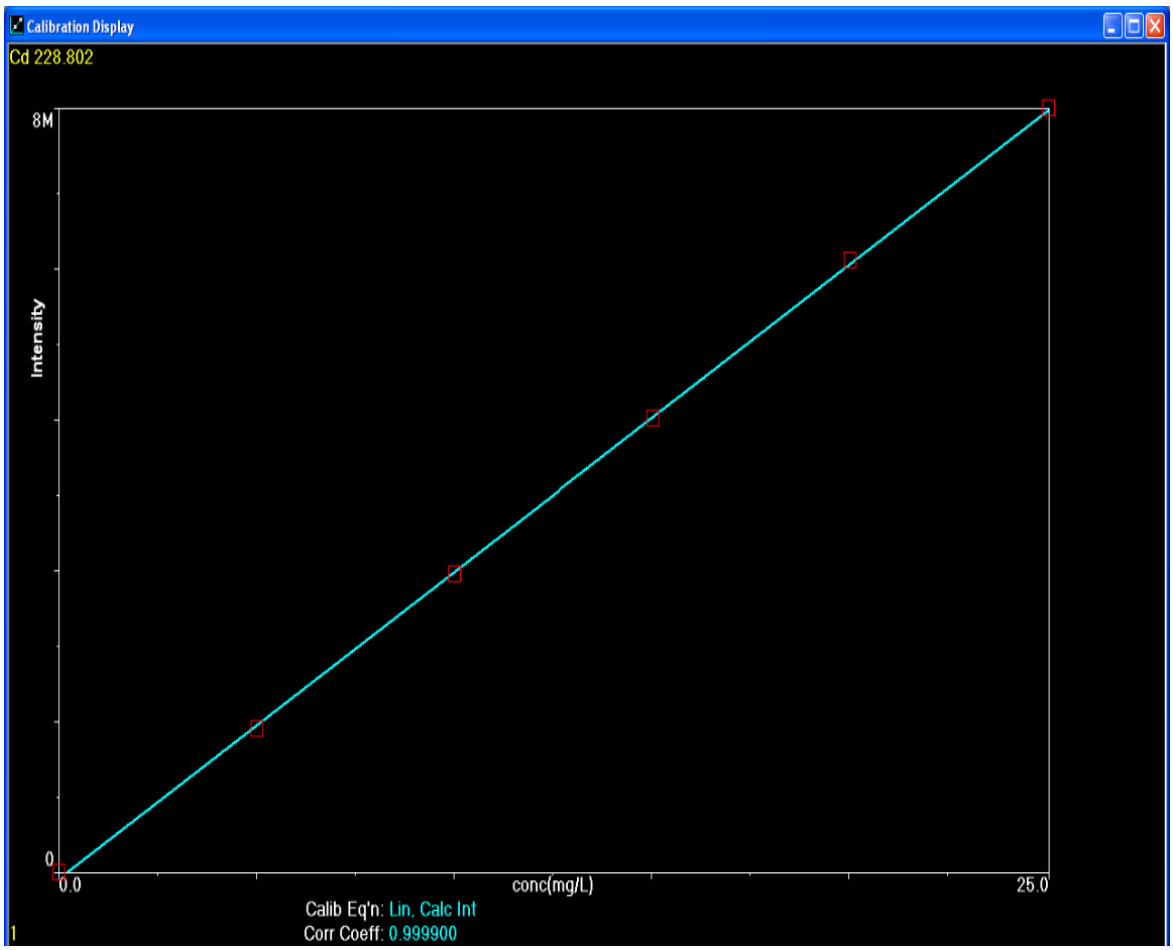

APPENDIX D: Sample Calculation for the Preparation of 0.1 M of HCl

Sample calculation for the preparation of 0.1 M of HCl

Given:

Molecular Weight of HCl = 36.5 g/mol

Specific gravity of 37 wt% HCl = 1190 g/L

Molarity of 37 wt% HCl

$$\frac{37\text{ ml}}{100\text{ ml}} \text{x} 1190\ \frac{\text{g}}{\text{L}}\ \text{x}\ \frac{1}{36.5\ \frac{\text{g}}{\text{mol}}} = 12.06\ \text{M}$$

By using dilution factor equation to obtain the amount of 12.06 M of HCl to be diluted to achieve 0.1 M of HCl.

$$C_1V_1 = C_2V_2$$

where,

C_1 = 12.06 M

C_2 = 0.1 M

V_1 = volume of 37 wt% HCl required for dilution, mL

V_2 = 500 mL

$$V_1 = \frac{C_2V_2}{C_1}$$

$$= \frac{0.1\text{ M x }500\text{ mL}}{12.06\text{ M}}$$

= 4.146 mL

So, 4.146 mL of 37 wt% HCl is needed to mix with 495.854 mL of distilled water in order to produce 0.1 M of HCl.

APPENDIX E: Sample Calculation for the Preparation of 0.1 M NaOH

Sample calculation for the preparation of 0.1 M of NaOH

Given:

Molecular Weight of NaOH = 40 g/mol

Volume of 0.1 M of NaOH = 500 mL / 0.5 L

$$0.5 \text{ L x } 0.1 \ \frac{\text{mol}}{\text{L}} \text{ x } 40 \ \frac{\text{g}}{\text{mol}} = 2 \text{ g}$$

So, 2 g of solid pellet NaOH is required to mix with 500 mL of distilled water in order to produce 0.1 M of NaOH.

APPENDIX F: FTIR Spectrum of Neat PSF

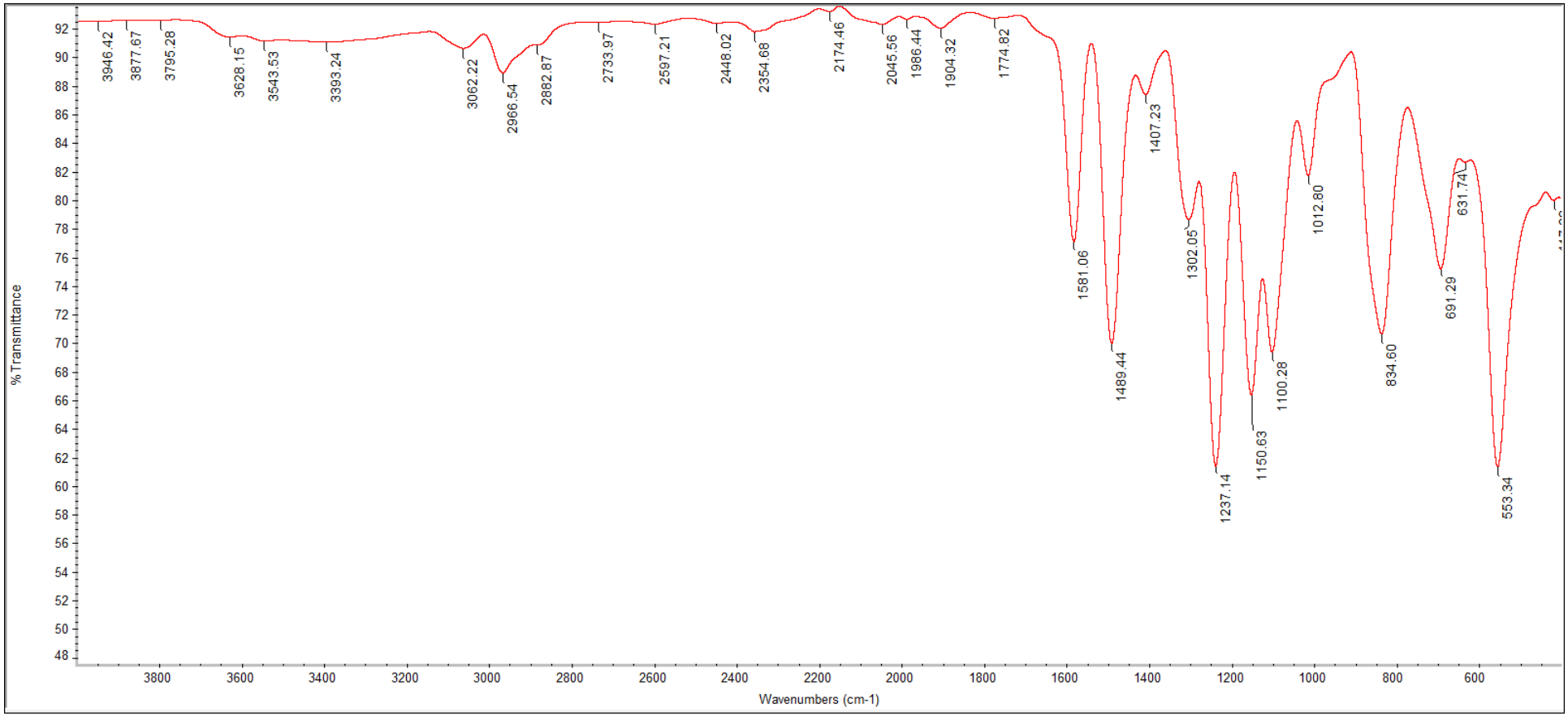

APPENDIX G: FTIR Spectrum of 1 wt% ZnO/GO MMM

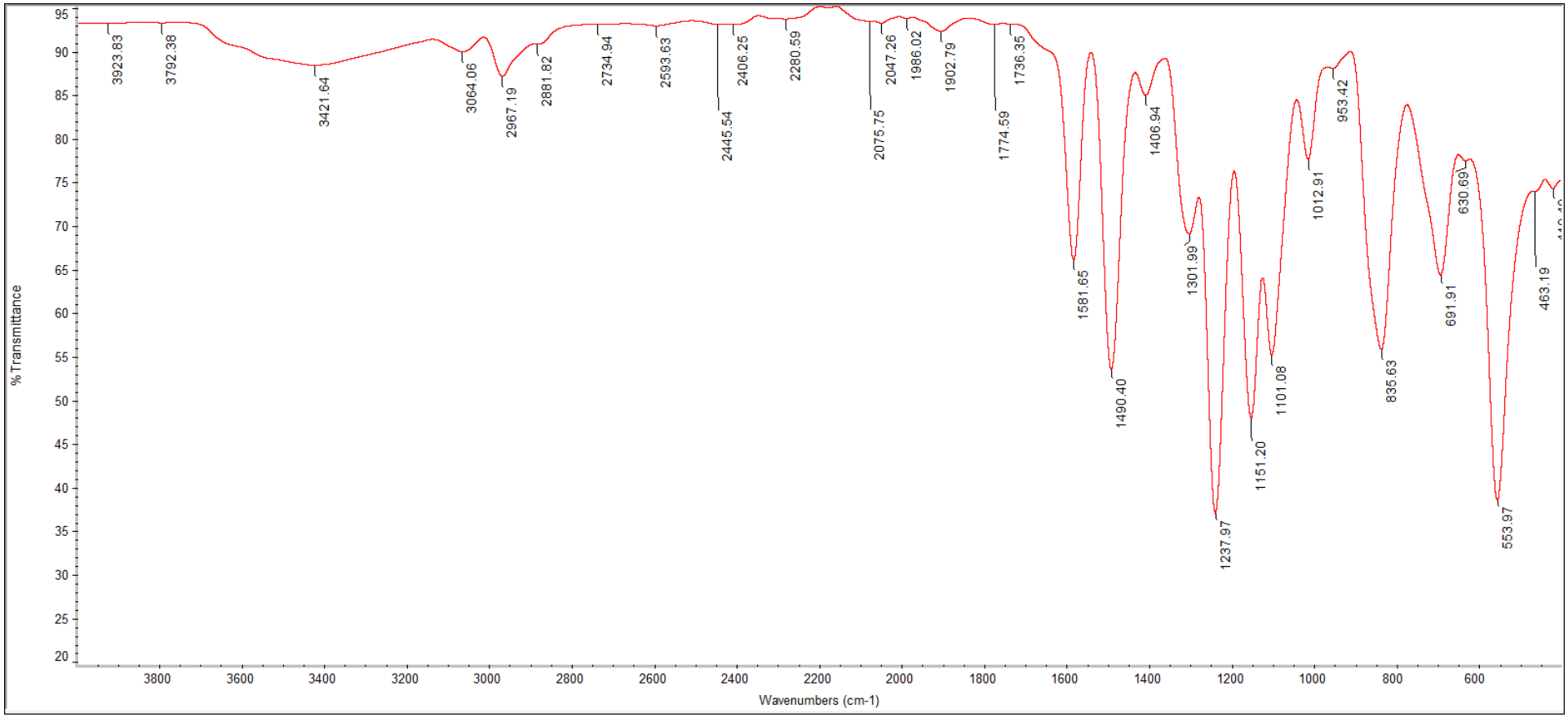

APPENDIX H: Sample Calculation for Adsorption Capacity, q_e at pH of 5.5

Sample calculation for adsorption capacity, q_e at pH of 5.5

$$q_e = \frac{(C_o - C_e)V}{m}$$

where,

C_o = 27.55 mg/L

C_e = 26.88 mg/L

V = 0.01 L

m = 7 cm^2

$$q_e = \frac{\left(27.55\ \frac{mg}{L} - 26.88\ \frac{mg}{L}\right)0.01\ L}{7\ cm^2}$$

$$= 0.000957\ \frac{mg}{cm^2}$$

APPENDIX I: Sample Calculation for Adsorption Capacity at time *t*, q_t for 3 hours Contact Time

Sample calculation for adsorption capacity at time *t*, q_t for 3 hours contact time

$$q_t = \frac{(C_o - C_e)V}{m}$$

where,

C_o = 28.10 mg/L

C_e = 27.72 mg/L

V = 0.01 L

m = 7 cm^2

$$q_e = \frac{\left(28.10\ \frac{mg}{L} - 27.72\ \frac{mg}{L}\right)0.01\ L}{7\ cm^2}$$

$$= 0.000543\ \frac{mg}{cm^2}$$

APPENDIX J: Sample Calculation for Difference Per Membrane (ppm) and Adsorption Per Area Membrane (ppm/cm^2) (5 membranes)

Sample calculation for difference per membrane (ppm) and adsorption per area membrane (ppm/cm^2) (5 membranes)

Difference in concentration before and after adsorption = 2.67 ppm

Difference per membrane = $\frac{2.67}{5} = 0.534$ ppm

Adsorption per area membrane = $\frac{0.534 \text{ ppm}}{7 \text{ cm}^2} = 0.0763 \frac{\text{ppm}}{\text{cm}^2}$

APPENDIX K: Results Generated from the ICP-OES for Different Number of Membranes

Mean Data: 1

Analyte	Mean Corrected Intensity	Calib. Conc.	Units	Std.Dev.	Sample Conc.	Units	Std.Dev.	RSD
Cd 228.802	8455572.8	25.89	mg/L	0.027	25.89	mg/L	0.027	0.10%

Mean Data: 2

Analyte	Mean Corrected Intensity	Calib. Conc.	Units	Std.Dev.	Sample Conc.	Units	Std.Dev.	RSD
Cd 228.802	8248365.7	25.26	mg/L	0.153	25.26	mg/L	0.153	0.60%

Mean Data: 3

Analyte	Mean Corrected Intensity	Calib. Conc.	Units	Std.Dev.	Sample Conc.	Units	Std.Dev.	RSD
Cd 228.802	8107336.2	24.83	mg/L	0.113	24.83	mg/L	0.113	0.46%

Mean Data: 4

Analyte	Mean Corrected Intensity	Calib. Conc.	Units	Std.Dev.	Sample Conc.	Units	Std.Dev.	RSD
Cd 228.802	7990630.1	24.48	mg/L	0.038	24.48	mg/L	0.038	0.15%

Mean Data: 5

Analyte	Mean Corrected Intensity	Calib. Conc.	Units	Std.Dev.	Sample Conc.	Units	Std.Dev.	RSD
Cd 228.802	7718378.2	23.65	mg/L	0.064	23.65	mg/L	0.064	0.27%

APPENDIX L: Sample Calculation for Percentage of Regeneration at Cycle 3

Sample calculation for percentage of regeneration at cycle 3

Difference in concentration before and after adsorption = 0.38 ppm

Percentage of regeneration = $\frac{0.38}{0.42} x\ 100\%$ = 90.48%

APPENDIX M: Sample Calculation for Amount of Adsorbed Cd^{2+} Per Weight of ZnO/GO

Sample calculation for amount of adsorbed Cd^{2+} per weight of ZnO/GO

For adsorbed Cd^{2+} in membrane per weight of ZnO/GO

where,

Average adsorbed Cd^{2+} = 0.49 ppm (from section 4.2.4)

Total membrane area = 780 cm^2 (3 x 20 cm x 13 cm)

Weight of ZnO/GO that had been used in casting membranes = 0.1 g

Weight of ZnO/GO for 7 cm^2 of membrane = $\frac{0.1 \text{ g x } 7 \text{ cm}^2}{780 \text{ cm}^2}$ = 0.0008974 g

Adsorbed Cd^{2+} in membrane per weight of ZnO/GO = $\frac{0.49 \text{ ppm}}{0.0008974 \text{ g}}$ = 546.02 ppm/g

0.1 g of ZnO/GO was used to cast membranes that had 780 cm^2 (3 x 20 cm x 13 cm) and 0.0008974 g of ZnO/GO existed in 7 cm^2 of membrane by assuming the casting solution is homogenous. Hence, the adsorbed Cd^{2+} in membrane per weight of ZnO/GO was 546.02 ppm/g by using 0.49 ppm of average adsorbed Cd^{2+}.

For adsorbed Cd^{2+} in bulk per weight of ZnO/GO

where,

Initial Cd^{2+} concentration = 92.53 ppm

Final Cd^{2+} concentration = 42.63 ppm

Difference in Cd^{2+} concentration = 92.53 ppm – 42.63 ppm

= 49.9 ppm

Weight of ZnO/GO that had been used = 0.13 g

Adsorbed Cd^{2+} in bulk per weight of ZnO/GO = $\frac{49.9 \text{ ppm}}{0.13 \text{ g}}$ = 383.85 ppm/g